



HAL
open science

A novel quantile regression approach to define optimal ecological niche: a case study on habitat suitability of cockle populations (*Cerastoderma edule*)

Amélie Lehuen, Chloé Dancie, Florent Grasso, Sven Smolders, Francesco Cozzoli, Francis Orvain

► To cite this version:

Amélie Lehuen, Chloé Dancie, Florent Grasso, Sven Smolders, Francesco Cozzoli, et al.. A novel quantile regression approach to define optimal ecological niche: a case study on habitat suitability of cockle populations (*Cerastoderma edule*). 2024. hal-04438267v2

HAL Id: hal-04438267

<https://normandie-univ.hal.science/hal-04438267v2>

Preprint submitted on 13 Nov 2024

HAL is a multi-disciplinary open access archive for the deposit and dissemination of scientific research documents, whether they are published or not. The documents may come from teaching and research institutions in France or abroad, or from public or private research centers.

L'archive ouverte pluridisciplinaire **HAL**, est destinée au dépôt et à la diffusion de documents scientifiques de niveau recherche, publiés ou non, émanant des établissements d'enseignement et de recherche français ou étrangers, des laboratoires publics ou privés.



Distributed under a Creative Commons Attribution - NonCommercial 4.0 International License

A NOVEL QUANTILE REGRESSION APPROACH TO DEFINE OPTIMAL ECOLOGICAL NICHE: A CASE STUDY ON HABITAT SUITABILITY OF COCKLE POPULATIONS (*CERASTODERMA EDULE*)

Amélie Lehuen^{a*}, Chloé Dancie^b, Florent Grasso^c, Sven Smolders^d, Francesco Cozzoli^e, Francis Orvain^a

^a Biologie des Organismes et Ecosystèmes Aquatiques (BOREA) Université de Caen Normandie UNICAEN, Sorbonne Université, MNHN, UPMC Univ Paris 06, UA, CNRS 8067, IRD, Esplanade de la paix, F-14032 Caen, France

^b CSLN, Cellule de Suivi du Littoral Normand (CSLN), 53 rue de Prony, 76600 Le Havre, France

^c Ifremer, DYNECO/DHYSED, F-29280 Plouzané, France.

^d Flanders Hydraulics Research, dept. of Mobility and Public Works, Flemish Government

^e es. Inst. on Terrestrial Ecosystems (IRET) – National Research Council of Italy (CNR) URT Lecce, Palazzina B - Complesso Ecotekne, via Monteroni 165, 73100 Lecce (LE) - Italia

* Corresponding author: amelie.lehuen@gmail.com

Abstract

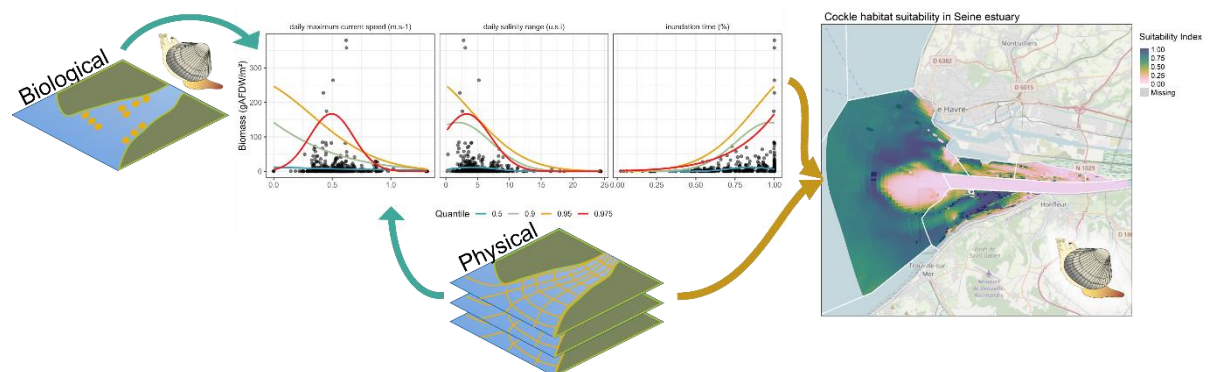
Correlative Species Distribution Models (SDMs) are powerful tools for understanding the spatial structure of ecological patterns and serve as a foundation for predicting the short-term effects of environmental changes on biological populations and for improving ecosystem management. However, due to complex and often non-linear interactions between biotic and abiotic factors, as well as irregular data distributions, SDMs are notoriously challenging to construct and validate, highlighting the need for continued research and methodological advancements in this active field of study. Quantile regression is a promising statistical technique to improve SDM as it can deal with data heteroskedasticity and provide a description of habitat suitability consistent with Liebig's Law of the Minimum. The aim of this study is to propose a tool for assessing habitat suitability of an estuary for a species, by defining its optimal ecological niche, which can be used for estuarine management, with a study case of *Cerastoderma edule* in the Seine estuary. The method involved applying quantile regression to a 20-year biological dataset coupled with a hydro-morpho-sedimentary model data set validated over a 25-year period, both at the scale of the estuary. To account for the complex distributional shapes, this study was carried out comparing three different types of equation (linear, Gaussian and B-spline). On the basis

32 of a preliminary multivariate analysis of the physical descriptors, two models were built representing
 33 hydrodynamic, morphodynamical and sedimentary features: daily maximum current speed, inundation
 34 time and daily salinity range or mud content as a third predictor. The Gaussian quantile regression
 35 produced the best description of the optimal niche, at the 97.5th centile and using the biomass. The
 36 optimal ecological niche for *C. edule* appeared to be lower intertidal marine areas, with low current
 37 speed, low salinity fluctuation and a sediment bed composed of muddy sand in the Seine estuary. The
 38 calculation of suitability index in this ecosystem was explored over a period of 25 years and analysed in
 39 isolated sectors to be applied in different scenarios related to global warming. The model using daily
 40 maximum current speed, inundation time and daily salinity range was also applied to data from the
 41 Scheldt basins, to test the reliability of the model, thus demonstrating that the model performs quite well,
 42 even though there were some differences of habitat suitability between these estuaries. This approach
 43 can allow direct comparisons of SDMs with one single Gaussian model and may offer new perspectives
 44 to investigate SDMs on a large scale.

45 Highlights

- 46 • Gaussian quantile regression at the 97.5th centile was the most performant model to define the
 47 optimal ecological niche of *C. edule* at the scale of the Seine estuary.
- 48 • Daily maximum current speed, inundation time and daily salinity range were the predictors the
 49 most adequate to build the optimal ecological niches.
- 50 • Optimal *Cerastoderma edule* conditions corresponded to low intertidal marine shores,
 51 moderate current speed, low salinity fluctuations in muddy sand sediment.
- 52 • The best model applied to the Scheldt basins shows some differences in the definition of
 53 optimal habitat compared with the Seine.

54 Graphical abstract



55

56 Keywords

57 *Cerastoderma edule*, quantile regression, species distribution model, optimum ecological niches,
58 habitat suitability, cockle populations, estuaries

59 Manuscript

60 1 Introduction

61 A species distribution model (SDM) is an approach that provides practical information on the spatial
62 distribution of species based on ecological niche modelling (ENM) by investigating correlative interaction
63 to predict the occurrence or the abundance of species as function of predictor variables. An ENM is
64 defined in an n-dimensional environmental space that can be geographically projected as a SDM,
65 providing managers and decision-makers with information about species distribution to help
66 stakeholders to define conservation plans (Austin, 2007, 2002). A wide choice of statistical models for
67 constructing SDM is available, with two main categories: the correlative ones (Austin, 2002; Guisan and
68 Zimmermann, 2000) and the mechanistic ones (Kearney and Porter, 2009), the latter being based on
69 eco-physiological laws. Each approach has advantages and disadvantages (Kearney and Porter, 2009;
70 Melo-Merino et al., 2020), but the vast majority of studies carried out to date are correlative (Melo-Merino
71 et al., 2020; Robinson et al., 2011, 2017).

72 Correlative SDMs link the presence-absence or population quantitative information (abundance,
73 biomass) of a targeted species with spatio-temporal habitat data, thereby quantifying the relation
74 between environmental factors and species distribution (Elith and Leathwick, 2009; Franklin, 2010;
75 Guisan and Thuiller, 2005). These methods generally use geo-localised biological data of a species and
76 abiotic parameters measured by techniques such as remote measurements or modelling (Brown et al.,
77 1996; Guisan and Zimmermann, 2000; Melo-Merino et al., 2020; Van Der Wal et al., 2008).

78 Correlative SDMs encompass a multiplicity of statistical techniques, which can be divided into two
79 approaches: algorithmic modelling (AM) and data modelling (DM) (Warren and Seifert, 2011). AM
80 methods, such as MaxEnt or random forest, involve a statistical comparison of abiotic and biological
81 data, without defining the type of relationship, embracing the overall intrinsic complexity of the
82 environment, with the aim of maximum prediction performance, but without describing the physiological
83 processes involved. These methods have recently undergone considerable development, thanks to the
84 increasingly easy access to the computer tools needed to implement them, they have been applied for
85 instance on cockle populations (Matos et al., 2023; Singer et al., 2017). The DM approach, which is
86 more historical, consists of defining *a priori* a type of relationship between abiotic factors and biological
87 response, based on the state of the art of the species and its environment, in a principle of parsimony
88 and simplification of the description of an environment. The aim is then to highlight the main physiological

89 processes explaining population dynamics, and to provide tools that can be applied in spatially and
90 temporally diverse contexts.

91 In the context of a DM approach, various regressions techniques can be used, which are often based
92 on Ordinary Least Squares (OLS), which defines the conditional mean function between the biological
93 response and selected predictors (Koenker and Hallock, 2000). Whatever the number of factors used,
94 there will always be unmeasured or unknown factors, which may have a limiting effect on the biological
95 response, which then reflects the response to these unknown limiting factors. This is the statement of
96 Liebig's law of minima: if other resources are not optimal for some observations, the measured response
97 of the species will be lower than the maximum possible response to the recorded resource (Anderson,
98 2008; Cade and Noon, 2003). This generates heteroskedasticity in bivariate or multivariate data
99 distributions, as the mean and variance of the species abundances along environmental gradients tend
100 to be positively correlated, thereby violating one of the fundamental assumptions of OLS modelling. It
101 follows that the construction of a OLS-based SDM cannot take into account all meteorological,
102 hydrodynamic, morphological or sedimentary factors, such as the patchy spatial distribution of many
103 species, variations in recruitment from one year to the next, and the complex life cycles of some species
104 (Ysebaert and Herman, 2002) that may partly bias the biological response to a set of selected factor
105 (Austin, 2007; Cade et al., 1999).

106 The use of quantile regression (QR) can counteract this limitation, by defining different quantiles of
107 biological response depending on the abiotic factors chosen (Koenker and Hallock, 2000; Koenker and
108 Machado, 1999). Studies have been conducted for more than 40 years to apply QR, and recent
109 advances in computer tools have improved its use and facilitated its interpretation especially for
110 ecological applications, such as SDM (Austin, 2007; Cade et al., 2005, 1999; Cade and Noon, 2003;
111 Jiménez-Valverde et al., 2021). The variability of the biologic response to a fixed environmental condition
112 could be considered to reflect the expression of other more or less limiting factors. By targeting the
113 upper quantiles in a QR, it is possible to define the best maximum biological response to selected abiotic
114 predictors, with any other factors, whether biological, environmental or mobility being considered as
115 non-limiting (Schröder et al., 2005). In other words, while classical ENM focus on modelling the average
116 response to the environment, QR ENM focus more on modelling extremes, thus providing a description
117 of species abundance distribution consistent with the theoretical principle of Liebig's Law. The modelling
118 of extremes, if based on a sufficiently rich dataset (over the long term, in various environmental
119 conditions), has the potential to outline the boundaries of species niches, describing what we named
120 Optimal Ecological niche (OEN), by removing particular conditions recorded (meteorological conditions,
121 sanitary events, lifespans).

122 This type of OEN can be a key tool for estuarine and coastal management in the context of climate
123 change and anthropogenic pressures (Crossland et al., 2005; Grassle, 2013). Indeed, understanding
124 the links and interactions between abiotic and biotic components is necessary to preserve biodiversity
125 and restore areas affected by environmental fluctuations and human activity, in order to conserve the
126 benefits of their functional ecosystem services (Richards and Lavorel, 2023). Among a vast list of
127 ecosystem services, an estuary is a shipping lane, a fishing ground and an area comprising diverse

128 natural habitats (Hughes et al., 2014). All these activities compete for space and have different needs
129 and yet are linked to each other, so it is necessary to have decision support tools that improve their
130 management and enable their future development (Degraer et al., 2008; He et al., 2015; Schickele et
131 al., 2020). In particular, the vulnerability of estuarine sediments to the sea level increase and coastal
132 squeeze has been identified for a long time with a strong negative impact on the trajectory of tidal flats
133 (Healy et al., 2002; Murray et al., 2019). Many studies highlight the relevance of ecological gradients in
134 estuaries (Brown et al., 1996; Guarini et al., 1998; Van Der Wal et al., 2010), where intertidal areas are
135 undeniably subject to massive and frequent gradients, due to both actions of the tide and the river
136 discharge, modifying the physico-chemical environment of water bodies. Physical gradients drive the
137 set of interaction links with fauna in estuaries (Chapman et al., 2010, p. 20; Herman et al., 2001).

138 Within estuarine fauna, benthic macrofauna (or macrozoobenthos) is a key element in ecosystem
139 functioning. Often primary consumers, they are a source of trophic support for the higher levels, in
140 particular for fish and shorebirds (Saint-Béat et al., 2013). Their presence on or in the sediment
141 contributes to sediment biogeochemical fluxes and morphological dynamics of their environment
142 through a series of eco-engineering processes (Arlinghaus et al., 2021; Jones et al., 1994; Kristensen
143 et al., 2012). The capacity of benthic macrofauna to resist external stressors is yet not fully understood,
144 but abiotic factors are habitat-defining parameters on which a cohort of species depends (Ysebaert and
145 Herman, 2002). In particular, sediment and hydrological parameters have a direct impact on the activity
146 and spatial distribution of macrozoobenthos, with sediment acting as a food source, habitat, shelter and
147 breeding ground but which can also cause discomfort and stressful conditions (erosion, mud
148 accumulation, anoxic episodes...). Sediment indicators, including grain size median and fine silt content,
149 have been shown to strongly contribute to explaining variations in macrozoobenthic communities
150 (Anderson, 2008; Thrush et al., 2005, 2003). It is therefore very relevant to focus on the response of
151 macrozoobenthos not only to temperature or salinity changes, but also to physical dynamics occurring
152 in an estuary (Shi et al., 2020; Van Der Wal et al., 2017) such as sea level rise, increases in wave and
153 current intensity related to more frequent storms or also the risk of coastal squeeze.

154 The benthic macrofauna of the Seine Bay (Normandy, France) has been extensively studied in recent
155 decades (Bacouillard et al., 2020; Baffreau et al., 2017; Dauvin, 2015; Le Guen et al., 2019) and
156 estuarine management included in subsequent regional program frameworks ([https://www.seine-
157 aval.fr/](https://www.seine-aval.fr/)). Accessing abiotic factors, and especially physical forcings, in an estuary is a challenge that can
158 be solved by developing hydro-morpho-sedimentary (HMS) models, which use principles of fluid and
159 particle physics to define the parameters of interest in the estuary at an intermediate scale. The Seine
160 estuary (Normandy, France) was the subject of the Mars3D model adjustment, which describes the
161 dynamics of the physical parameters in an estuary, such as bottom elevation, salinity, temperature,
162 current velocity, water surface elevation, with a particular effort invested in describing the erosion,
163 deposition and consolidation properties of sand-mud mixtures (Grasso et al., 2021, 2018; Grasso and
164 Le Hir, 2019; Mengual et al., 2020; Schulz et al., 2018). Such tools allow temporal projection on a
165 regional spatial scale and therefore to develop climate-focused forecasts and scenarios. On the basis
166 of this available information, on both biological and abiotic components, it is then possible to model the

167 spatial distribution of the targeted species, in order to better define the fauna-environment interactions
168 that shape the presence and the performances of the species in the estuary under consideration.

169 Investigating populations of *Cerastoderma edule*, the common cockle, as an example in the Seine
170 estuary, the aim of this study is to assess the ENM following the principles of the DM approach, with the
171 biological response (biomass and density) as a function of the hydro-morpho-sedimentary factors of the
172 estuary extracted from a 3D model. With the aim of proposing an OEN transferable to other estuarine
173 environments, we used quantile regression at higher quantiles, with either linear or non-linear curve
174 responses (Gaussian and B-spline). While linear responses are the simplest, there's a danger of
175 oversimplifying species-environment relationships as in nature there are often "shortages" or
176 "surpluses". Furthermore, univariate linear relationship cannot account for the effect of subsidiary factors
177 the responses to which are inversely correlated with the variable of interest. For instance, the preference
178 of *C. edule* for the intermediate tidal flat can be intended as a combination between a positive response
179 to submersion time (longer feeding time) and negative response to increased current velocity
180 (dislocation). As a large number of subsidiary factors generally interact in shaping species distribution
181 along single gradients, Gaussian responses are useful for modelling species with a clear environmental
182 optimum, but still oversimplify the effect of interactions with co-varying subsidiary factors. Flexible shape
183 responses (like B-splines) provide a more nuanced view, capturing asymmetry in species responses to
184 environmental gradients, but less intuitive and more data-intensive. Building on the work done by
185 (Cozzoli et al., 2017, 2014, 2013), we propose to take the use of QR a step further by 1) showing that
186 using a Gaussian equation rather than a linear or B-spline equation is more appropriate to describe a
187 typical biological response, 2) building two models based on three environmental variables to reflect the
188 effects of hydrodynamic (including meteorological), morphological and sedimentary processes in an
189 estuary. These models were applied and analysed geographically in the Seine estuary, in the form of
190 suitability indices, as a tool for developing conservation and management plans. In addition, one of the
191 models was applied to an independent dataset from the Scheldt estuary (Cozzoli et al., 2014) in order
192 to discuss the transferability potential of an ENM for cockles at a more global scale.

193 2 Materials and Methods

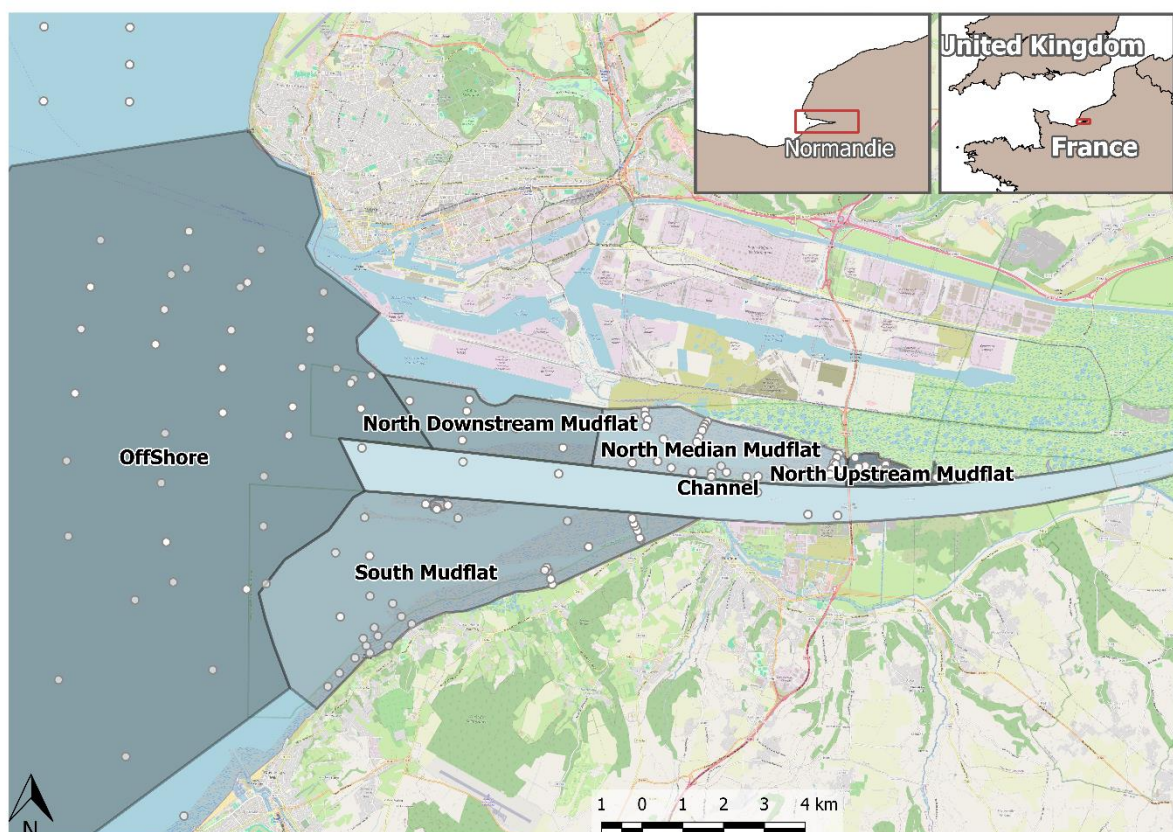
194 All data processing was conducted in R version 4.2.2 (2022-10-31 ucrt) except for Mars3D pre-
195 treatment in Matlab 2019a.

196 2.1 Study area

197 The Seine estuary in Normandy, north-west France, is defined as the last 170 km of the river leading
198 to the marine ecosystem close to Le Havre, starting at Poses weir upstream and ending in the bay of
199 Seine downstream. The Seine estuary is macrotidal (with a maximal tidal range of 8 m during spring
200 tides at Honfleur), and is subject to fresh water discharge ranging from 100 to more than 1000 m³.s⁻¹,
201 with a mean of 450 m³.s⁻¹ in the two last decades. Tidal dynamics and the wave regime have a significant
202 impact on the hydro-sedimentary dynamics of the mouth of the estuary (Grasso et al., 2021; Lesourd et
203 al., 2003; Schulz et al., 2018).

204 The mouth of the estuary hosts a variety of habitats that provide many ecosystem services (Beck et
205 al., 2001; Boesch and Turner, 1984). In particular, intertidal mudflats play a crucial role in the Seine
206 estuary and constitute areas of major interest including nutrient recycling, coastline protection, trophic
207 networks, nesting sites for migratory birds and fish nurseries. The Seine estuary is marked by artificial
208 structures that have profoundly modified this ecosystem, which is still undergoing changes that began
209 at the beginning of the 20th century (Lesourd et al., 2016). Numerous dykes were built and sediment
210 dredging was carried out to increase the capacity of the navigation channel, which contributed to the
211 disconnection of the two banks of the estuary and reduced the extent of wetlands, hence provoking a
212 “coastal squeeze”. Some of these works were large-scale projects: the construction of the Pont de
213 Normandie (1989-1995), which crosses the Seine estuary, and the “Port 2000” project (2000-2005) to
214 expand the port of Le Havre, mainly to give large container ships access to new all-day loading berths.

215 The Port 2000 project involved ecological compensation in the form of the creation of a nature
216 reserve in 1997, as well as the digging and dredging of an artificial channel in the north upstream mudflat
217 and the creation of a small island to serve as a resting place for migratory birds in the southern mudflat
218 (Aulert et al., 2009). Several historically known areas in the Seine estuary that differ in either their habitat
219 or community have been studied, mainly intertidal mudflats and subtidal areas (Morelle et al., 2020;
220 Tecchio et al., 2016) (Figure 1).



221
222 *Figure 1 Maps showing the habitats defined in the dataset of the study area. Dots represent the*
223 *location of the biological samples.*

224 2.2 Biological model

225 The cockle *Cerastoderma edule* (Linnaeus, 1758) is a bivalve belonging to the family of Cardiidae
226 that is widely distributed and exploited in waters off northern Europe to north Iceland and off the coast
227 of West Africa down to southern Senegal (Hayward and Ryland, 1995). The oval ribbed shells of the
228 cockle can reach 6 cm in diameter and are white, yellowish or brown in colour, and its lifespan is 2-3
229 years (Malham et al., 2012). Cockles are suspension-feeders, inhabiting the few uppermost centimetres
230 of the sediment with its two siphons emerging from the surface. Its growth depends mainly on
231 microphytobenthos in the juvenile stage and on phytoplankton in the adult stage (Sauriau and Kang,
232 2000). It provides numerous ecosystem services (Carss et al., 2020), and is a bioturbator species
233 actively studied for its effects on sediment morphology (Eriksson et al., 2017). Cockle habitats are
234 located in the central areas of the foreshore subject to medium currents (between 0.3 and 0.7 m.s⁻¹ of
235 maximum tidal current speed) (Herman et al., 1999; Ysebaert et al., 2002), typical marine salinity (> 30)
236 and they prefer fine sands (slightly silty, grain size between 100 and 200 µm) (Cozzoli et al., 2014;
237 Ubertini et al., 2012). This species can be found at particularly high densities in the English Channel,
238 the most densely inhabited area being the Bay of Veys, (density in the order of 200 to 500 ind.m⁻²), and
239 may exceptionally exceed 5000 ind.m⁻² (Gosling, 2003; Mahony et al., 2022). Winter conditions, current
240 intensity and stress (erosion) appear to explain the high mortality rates observed in some years (Herman
241 et al., 1999; Van Colen et al., 2010). Assessment of habitat suitability and SDM in previous studies
242 mainly report the relevance of submersion (Cozzoli et al., 2014; Matos et al., 2023; Singer et al., 2017),
243 salinity (Matos et al., 2023), temperature (Singer et al., 2017) and current velocity (Cozzoli et al., 2014).

244 2.3 Datasets

245 2.3.1 Biological data

246 Data concerning the benthic macrofauna of the Seine Bay are grouped in a database named
247 *MAcrobenthos Baie et Estuaire de Seine* (MABES) (Dauvin et al., 2006; L'Ebrelec et al., 2019). This
248 dataset provides information on sampling (geolocation, sampling method) and fauna (density [ind.m⁻²],
249 biomass [gAFDW.m⁻²] – Ash Free Dry Weight) collected in several projects for the past 40 years. This
250 database was completed with data from the *Cellule de Suivi du Littoral Normand* (CSLN) surveys
251 conducted for the *Maison de l'Estuaire*.

252 The raw data were harmonised and grouped in a single database which contains a total of 543
253 observations of *Cerastoderma edule*, and 86 sampling stations (with some variation in coordinates from
254 year to year), with an average of 24 stations sampled in each campaign (depending of the project),
255 mainly in September, October, and November. A series of 5-year periods was defined within the duration
256 covered by the dataset, from 2000 to 2019 (the years before 2000 were discarded as they contained
257 too few observations, n = 17): 2000-2005, including the construction of 'Port 2000' which caused major
258 disruptions in the estuary; 2006-2010; 2011-2015; 2016-2019. These periods correspond to identified
259 hydro-morphological sequences in the estuary.

260 2.3.2 Hydro-Morpho-Sedimentary data

261 The HMS model Mars3D can be used in the context of estuarine hydrodynamics and application to
262 fine sediment and sand transport. This three-dimensional (3D) process-based model was set up and
263 run under realistic forcings (including tide, waves, wind, and river discharge). The Mars3D model is
264 composed of the hydrodynamic core forced by the WAVEWATCHIII® wave model (Roland and Arduin,
265 2014) coupled with the MUSTANG sediment module (erosion, deposition, consolidation). This
266 MUSTANG module takes into account spatial and temporal variations in sand and mud content in the
267 multi-layered sediment bed, as well as consolidation processes, and also solves advection/diffusion
268 equations for different classes of particles in the water column (Grasso et al., 2018; Le Hir et al., 2011;
269 Mengual et al., 2020).

270 The HMS dataset was generated during the ARES project using the Mars3D model (Grasso et al.,
271 2021, 2019). The ARES dataset covers the simulation periods 1990-2000 and 2005-2018. The period
272 2001-2004 was not modelled because it corresponds to the period of construction of the Port 2000
273 project. The dataset outputs are available at intervals of 30 minutes for the entire Seine Bay area each
274 hydrological year, starting on October 1st and finishing on September 30th. The hydrological sub-data
275 contain 58 variables, some of which depend on water depth, with 10 levels in the water column, of which
276 only the median of the 3 lower layers were retained to reflect benthic conditions: current speed,
277 temperature, salinity and SPM for 5 particles sizes. Inundation rates were indirectly calculated from
278 bathymetry and water height of the model. The sedimentary sub-data contain 19 variables, some of
279 which depend on the depth in the sediment, with 6 levels corresponding to 1 m, of which only the median
280 of the 4 upper layers is retained, i.e. 10 cm to reflect benthic conditions: temperature, salinity and
281 sediment concentration for 5 particles sizes. The other retained variables retained were the total
282 thickness of the sediment and the bed shear stress. (Grasso et al., 2018) validated the Seine Estuary
283 model in terms of hydrodynamics, salinity, and SSC from tidal to annual time scales at different stations
284 within the estuary, the sediment fluxes were considered more qualitative (Grasso et al., 2021).

285 In addition to these variables, processing was carried out to extract supplementary information. The
286 daily maximum was calculated for current speed and bed shear stress. The daily range was calculated
287 for salinity and temperature and the yearly sediment budget was calculated from the variation in
288 sediment thickness at the beginning and end of the year. The sediment total concentration is the sum
289 of all sediment concentrations, and the mud content was deduced from the different particle size
290 concentrations. All the variables selected and created, 14 in all, were reduced to a median calculated
291 over the hydrological year. Biological data were associated with HMS variables corresponding to the
292 model cell and the relevant hydrological year according to the sampling date.

293 These 14 abiotic factors were studied to select the most relevant factors and limit their number in
294 order to avoid autocorrelations. A PCA (`FactoMineR::PCA` (Husson et al., 2024) and `factoextra`
295 (Kassambara and Mundt, 2020) package for visualisation) was carried out on all the factors, allowing
296 complementary parameters to be identified on the two main axes. In addition, a correlation matrix with

297 the biomass and density of *C. edule* ensure that there was no direct correlation between abiotic and
 298 biotic factors.

299 2.4 Model adjustments

300 2.4.1 Quantile regression

301 The mathematical theory of the quantile regression (QR) has been extensively expanded and
 302 described by Koenker over the past decades (Koenker, 2019; Koenker et al., 2019; Koenker and
 303 Bassett, 1978; Koenker and Hallock, 2000, 2001; Koenker and Machado, 1999). Its use in ecological
 304 studies has increased since the first pioneering studies (Cade et al., 2005, 1999; Cade and Noon, 2003).

305 In practice, correlative ENM with QR can use any type of equation that links abiotic factors to a
 306 biological response, with any number of predictors to be used. Yet it was observed that the biological
 307 response to physical factors is often non-linear, and can be modelled by a gaussian distribution
 308 (Huisman et al., 1993; Van Der Wal et al., 2008). With this in mind, we have defined three different types
 309 of models in this study (Table 1) to describe the interplay of three abiotic factors to the biological
 310 response, by testing different functions (linear, B-spline and Gaussian). Mathematical notation is based
 311 on (1) the τ subscript for variables that are quantile-dependent, (2) β for model coefficients, that are
 312 vectors of length τ , (3) μ and σ for mean and standard deviation. QR were performed with the `quantreg`
 313 package in R developed by (Koenker et al., 2024). The three model types were computed with different
 314 quantiles $\tau = [0.5, 0.9, 0.95, 0.975]$.

315 The model was adjusted on the biological data with the associated HMS data to create ENMs, which
 316 were then applied to the HMS data set, focused on the estuary. The maximum of each quantile of the
 317 ENM was used to standardise the model response, in order to create a suitability index, ranging from 0
 318 to 1. The results are displayed in maps with the mean of the model over each period, for each cell. A
 319 mean of the suitability index by area and period is calculated to visualise the global suitability over the
 320 whole estuary and the contribution of each factor.

321 *Table 1 List of types of models tested*

Type	Equation	Rationale
RQ linear with interaction	$y_{\tau} = \beta_{0\tau} + \beta_{1\tau} \cdot x_1 + \beta_{2\tau} \cdot x_2 + \beta_{3\tau} \cdot x_3$ $+ \beta_{4\tau} \cdot x_1 \cdot x_2 + \beta_{5\tau} \cdot x_2 \cdot x_3$ $+ \beta_{6\tau} \cdot x_1 \cdot x_3 + \beta_{7\tau} \cdot x_1 \cdot x_2 \cdot x_3$ <code>quantreg::rq(x1*x2*x3)</code>	Comparison with the results of a previous study (Cozzoli et al., 2014)
RQ gaussian (non-linear)	$y_{\tau} = A \cdot e^{-\left[\frac{(x_1 - \mu_{1\tau})^2}{2 \cdot \sigma_{1\tau}^2} + \frac{(x_2 - \mu_{2\tau})^2}{2 \cdot \sigma_{2\tau}^2} + \frac{(x_3 - \mu_{3\tau})^2}{2 \cdot \sigma_{3\tau}^2} \right]}$ <code>quantreg::nlrq(f(x1,x2,x3, initial.conditions))</code>	Providing μ and σ initiated by the mean and the standard deviation for each predictor (Huisman et al., 1993; Schröder et al., 2005).
RQ linear with B-Spline	<code>quantreg::rq(splines::</code> <code>bs(x1,degree=3,knots= median(x1)) +</code> <code>bs(x2,degree=3,knots= median(x2)) +</code> <code>bs(x3,degree=3,knots= median(x3)))</code>	Avoid pre-determined shape of the equation and the use of a flexible non-linear function (Cozzoli et al., 2013)

322 2.4.2 Model selection

323 QR model validation was based on the Akaike Information Criterion (AIC). This index evaluates the
324 performance of the model using the fewest possible predictors (Akaike, 1974), and was adapted to the
325 QR (Cade et al., 2005), named AICc. Following Koenker's recommendation, the R^1 , equivalent to OLS
326 R^2 developed by Koenker and Machado (Koenker and Machado, 1999), was not used (Koenker, 2006).

327 In addition to the AIC, the relationship between predicted and observed values was plotted to
328 establish a validation plot (Cozzoli et al., 2014). The whole dataset was sampled with random
329 replacement. The predicted (model output) data were discretized in 10 homogeneous classes based on
330 the predicted values and for each class, the correspondent sample quantile of the observed data was
331 calculated. To assess the validity of the modelled quantiles, a linear correlation was drawn for each
332 quantile between random-predicted and observed values.

333 3 Results

334 3.1 Description of the biological data set

335 The biological dataset for *C. edule* was split into four periods: 2000-2005 (n = 108), 2006-2010 (n =
336 155), 2011-2015 (n = 174), 2015-2019 (n = 106). The following treatment focussed on the mudflats
337 inhabited by *C. edule* (south mudflat (n = 218), north median mudflat (n = 198), north downstream
338 mudflat (n = 82), north upstream mudflat (n = 2). The differences in biomass and density are detailed
339 according to the period and the surface area concerned in Supp. Data 3.1.

340 3.2 Selection of the Hydro-Morpho-Sedimentary factors and their association

341 The selected predictors were observed during the same period and in the same area as the biological
342 data (Supp. Data 3.2). Spatio-temporal variations were specific to each factor:

- 343 • Daily maximum current speed [$m \cdot s^{-1}$]: the most dynamic area was the channel, with an average
344 of $1.05 \pm 0.21 m \cdot s^{-1}$. The northern upstream and median mudflats were subject to temporal
345 changes in the distribution of the current during the last period, which had an impact on their
346 overall average (upstream $0.43 \pm 0.34 m \cdot s^{-1}$; median $0.63 \pm 0.3 m \cdot s^{-1}$). The southern
347 mudflat presented the same hydrological conditions as offshore, at values between those of
348 the northern upstream and median mudflats.
- 349 • Inundation time [Proportion of the tidal cycle between 0 and 1 without unit]: The northern
350 upstream mudflat (0.4 ± 0.36) corresponded to the upper intertidal zones and showed
351 higher tidal locations than the median (0.7 ± 0.35) and downstream mudflats (0.93 ± 0.17).
352 There was a decrease in inundation time during the latest period in the northern upstream
353 mudflat. The southern mudflat (0.85 ± 0.27) showed a shorter inundation duration than the
354 northern downstream mudflat.

- 355 • Daily salinity range: This factor varied considerably over space and over time. On the offshore
356 and southern mudflats, the salinity varied little during the day. Strongly influenced by the
357 river, the channel salinity varied from 15 to 20 during the day, but with dampening over time.
358 The very dynamic variations in salinity in the three northern mudflats decreased after 2005.
- 359 • Mud content [%]: The northern upstream mudflat and channel areas were composed of sandy
360 mud sediment (north upstream mudflat 42 +/- 30 %; channel 43 +/- 25 %) with increasing
361 mud content in the channel over time. The others are muddy sands (21 +/- 1%), with
362 decreasing mud content over time. Mud distribution was heterogeneous in all areas,
363 particularly in the northern upstream mudflat.

364 The PCA analysis on physical descriptors (Figure 2, Supp Data 3.2, detailed scores Table 2) gives
365 3 main dimensions for a total variance of 65.4 % (PC1 = 28.8 %, PC2 = 20.7 %, PC3 = 15.9 %):

- 366 • PC1 corresponded to the hydrodynamic forcing of the area with the contributions of the
367 following variables: daily maximum current speed (19.6 %), average current speed (17.8 %),
368 daily salinity range (17.8 %), daily maximum bottom shear stress (10.9 %), SPM (9.2 %),
369 average bed shear stress (8.7 %).
- 370 • PC2 was related to the morphology of the estuary with the contributions of the following
371 variables: average inundation time (23.1 %), daily temperature range (20.4 %), average
372 bathymetry (19.9 %), average salinity (14 %), average temperature (8.3 %).
- 373 • PC3 was related to the sedimentary characteristics of the bed with the contributions of the
374 following variables: average sediment total concentration (30.2 %), average mud content
375 [$<63 \mu\text{m}$] (29 %), average bed shear stress (18 %), daily maximum bed shear stress (7.2 %).

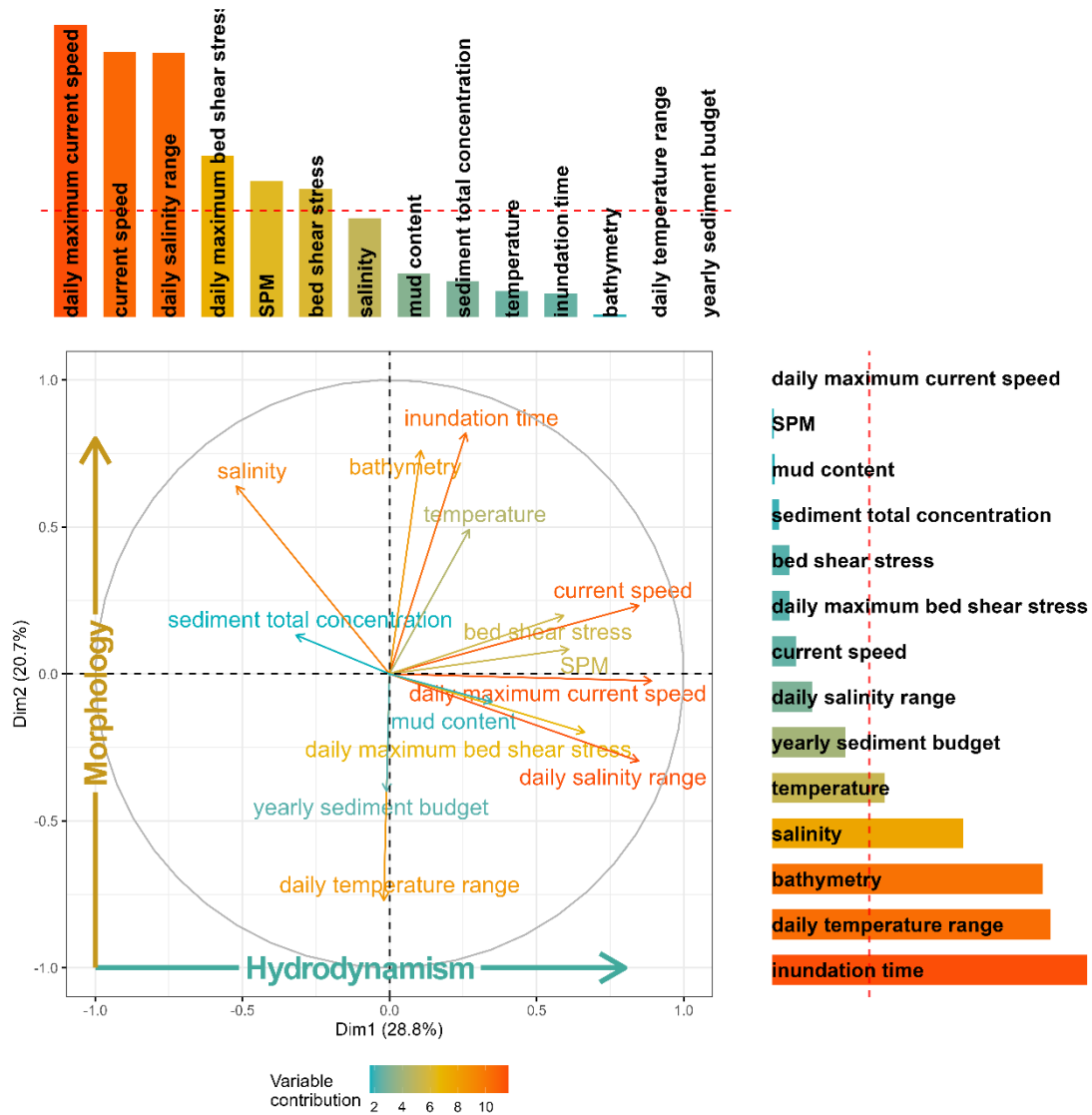
376 The PCA results were used to select predictors to capture the most relevant and transferable
377 variables. Considering those axes, two models were built with three abiotic factors:

378 A. Daily maximum current speed [$\text{m}\cdot\text{s}^{-1}$] & daily salinity range & inundation time [%] – PC1-PC1-
379 PC2: variables were the main contributors of the two first axes, but the third axis is not
380 represented at all. We have made this selection because these 3 predictors can be easily
381 retrieved at high frequency in other ecosystems or contexts. Those parameters are also
382 interesting because they contain information on the localisation of the tidal area that could
383 evolve with sea level rise and information on the hydrological conditions including river
384 floods, both processes in relation to climate change. The daily salinity range is a good
385 indicator of the estuarine condition, and have shown a high impact on *C. edule* patterns
386 (Matos et al. 2023). Moreover, this selection makes possible the direct comparison with a
387 previous study (Cozzoli et al., 2014).

388 B. Daily maximum current speed [$\text{m}\cdot\text{s}^{-1}$] & inundation time [%] & mud content [%] – PC1-PC2-
389 PC3: These factors represented the main contributors of the three first axes of the PCA.
390 Moreover, current speed and inundation time are easily measurable at high frequency
391 (Goberville et al., 2010). They illustrate three aspects of climate change potentially able to
392 alter spatial patterns of cockles: increase in storm-induced currents, global sea level rise and

393 general changes in sediment beds induced by erosion events that could be more frequent
 394 as a consequence of the global warming. Furthermore, the mud content could affect
 395 negatively *C. edule* habitability (Folmer et al., 2017).

396 There was no significant linear correlation between biological data and any of the environmental
 397 factors. Despite the high level of correlation and significance between biomass and density ($R =$
 398 0.866^{****}), these two variables were analysed in parallel.



399
 400 *Figure 2: Principal Components Analysis (PCA) variable correlation plot with the abiotic factors'*
 401 *contributions in bar plots for each axis. The red dotted line represents the mean contribution for all*
 402 *factors.*

403 *Table 2 Principal Components Analysis (PCA) scores for abiotic factors. Cos2, cosine squared of the*
 404 *variables, represents the quality of the representation of the variables on the PCA graph; Contribution*
 405 *represents the contributions (in percentage) of the variables to the principal components. The*
 406 *contribution of a variable to a given principal component: (Variable.cos2 * 100) / (total cos2 of the*
 407 *component).*

Variable	Cos2			Contribution		
	PC1	PC2	PC3	PC1	PC2	PC3
inundation time	0.07	0.67	0.00	1.67	23.10	0.13

current speed	0.72	0.05	0.01	17.82	1.86	0.46
daily maximum current speed	0.79	0.00	0.01	19.65	0.02	0.42
salinity	0.27	0.41	0.03	6.71	14.04	1.23
daily salinity range	0.72	0.09	0.00	17.78	3.02	0.13
temperature	0.07	0.24	0.02	1.83	8.31	1.00
daily temperature range	0.00	0.59	0.01	0.01	20.44	0.52
SPM	0.37	0.01	0.13	9.18	0.24	5.68
bathymetry	0.01	0.58	0.13	0.28	19.88	5.66
yearly sediment budget	0.00	0.16	0.01	0.00	5.47	0.38
bed shear stress	0.35	0.04	0.40	8.68	1.35	17.99
daily maximum bed shear stress	0.44	0.04	0.16	10.88	1.36	7.25
sediment total concentration	0.10	0.02	0.67	2.51	0.60	30.19
mud content	0.12	0.01	0.64	3.00	0.31	28.96

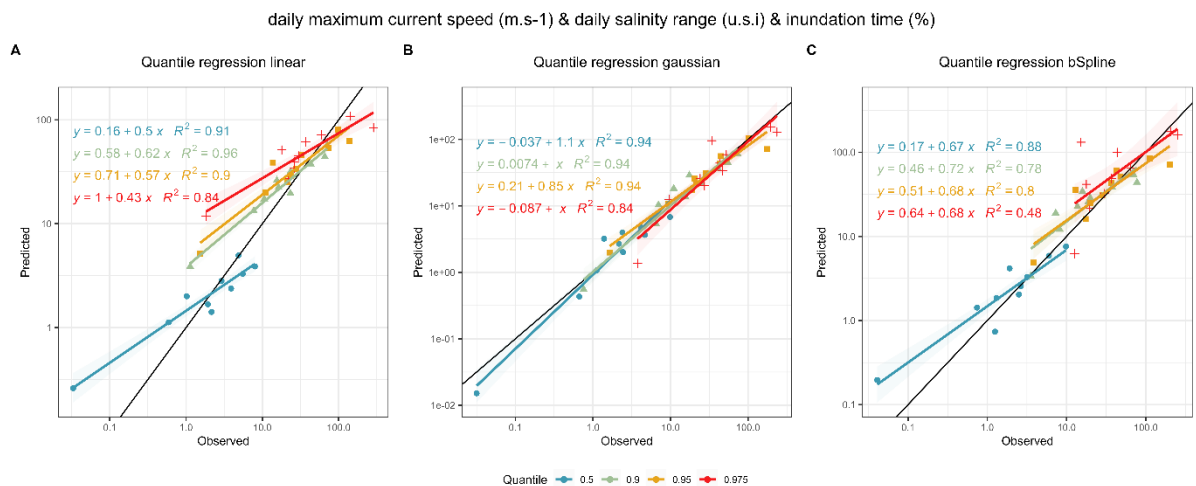
408 3.3 Model selection and validation

409 ENMs were computed using the three equations (linear, Gaussian and B-spline) for each
410 combination of abiotic factors at four selected quantiles ($\tau=0.5, 0.9, 0.95$ and 0.975). The best scores
411 were obtained for the biomass models compared to the density models, regardless of quantile. On
412 average, the AICc of the quantile regression with the Gaussian equation model were systematically
413 lower than the others for biomass (Table 3).

414 The validation plots comparing observed and predicted values (Figure 3), completed the
415 observations of AICc, i.e. Gaussian > B-Spline > linear (the regression lines of each quantile were closer
416 to the 1:1 line). The Gaussian equation performs best at the 97.5th percentile, since this is the highest
417 quantile calculated with the slope of the regression line between the predicted value and the observed
418 value closest to the 1:1 diagonal. We have therefore chosen to retain the 97.5th percentile as the optimal
419 quantile for subsequent analyses.

420 *Table 3 AICc comparison for all models computed, according to the quantile, the type of equation*
421 *and the response. In bold, the lower value of each model by response and quantile.*

	Biomass (gAFDW/m ²)				Density (ind/m ²)			
	0.5	0.9	0.95	0.975	0.5	0.9	0.95	0.975
daily maximum current speed (m.s-1) & daily salinity range & inundation time (%)								
Quantile regression bSpline	3858.7	4933.4	5297.1	5668.9	6977.6	8065.7	8403.0	8634.6
Quantile regression Gaussian	3835.0	4871.2	5240.9	5655.3	6969.1	8102.2	8476.1	8783.3
Quantile regression linear	3869.9	4918.5	5292.3	5702.6	6985.0	8067.4	8404.4	8706.1
daily maximum current speed (m.s-1) & inundation time (%) & mud content (%)								
Quantile regression bSpline	3745.4	4790.6	5148.1	5496.5	6758.8	7794.7	8126.5	8283.2
Quantile regression Gaussian	3733.7	4746.8	5071.5	5418.7	6745.2	7819.8	8186.1	8533.3
Quantile regression linear	3757.0	4794.8	5162.0	5527.7	6767.1	7815.0	8142.6	8361.2



422

423 *Figure 3: Example of modelled vs observed biomass data plotted for each model functions. The*
 424 *selected predictors were the daily maximum current speed [m.s⁻¹], daily salinity range and inundation*
 425 *time [% in this example]. The black line represents the 1:1 ratio, quantiles 0.5 in blue, 0.9 in green,*
 426 *0.95 in orange and 0.975 in red.*

427 3.4 Optimal ecological niche

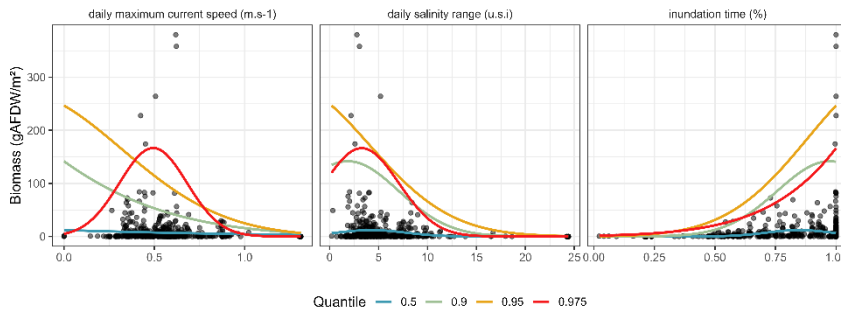
428 3.4.1 Quantile Regression with Gaussian equation

429 The modelled responses for each ENM quantile are represented by a projection on one axis per
 430 predictor with the observed data to observe the univariate effects of each variable (Figure 4 A1 & B1).
 431 The observed distribution of cockle biomass was left skewed, with a majority of records at low biomass
 432 values, and rare high biomass values, reflecting the validity of the choice of QR models. In addition,
 433 records were observed all along the environmental gradients of the selected predictors. The maximum
 434 observed responses located above the upper envelope of the model at $\tau=0.975$ are close to the model
 435 optimum. Furthermore, the two models can clearly be applied without any preference in terms of
 436 robustness, given the performance shown by the predicted/observed graph (Figure 4 A2 & B2), where
 437 we can see that the 97.5th percentile has a slope of 1 and a high R^2 in both models. The models using
 438 density showed the same results (Supp. Data 3.4.1). The coefficients of the models are displayed in
 439 Table 4, and optimum for each model is described in the range of predictors encompassing the realised
 440 biomass:

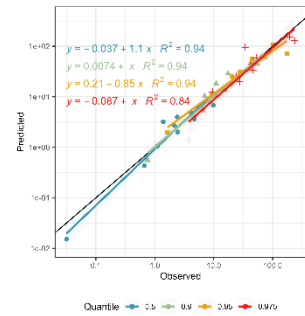
441 A. Daily maximum current speed [m.s⁻¹] & daily salinity range & inundation time [%] (Figure 4 A1
 442 & A2): The optimum was of 167 gAFDW.m² at 0.48 m.s⁻¹, with a range of 3.16 unity of salinity
 443 and 100 % inundation time. The optimum niche is a low intertidal zone with calm waters,
 444 where salinity is quite stable.

445 B. Daily maximum current speed [m.s⁻¹] & inundation time [%] & mud content [%] (Figure 4 B1 &
 446 B2): The optimum was of 239 gAFDW.m² at 0.43 m.s⁻¹, 100% inundation time and 31% of
 447 mud content. The optimal niche corresponds to low intertidal zones, with calm waters and
 448 muddy sands sediment.

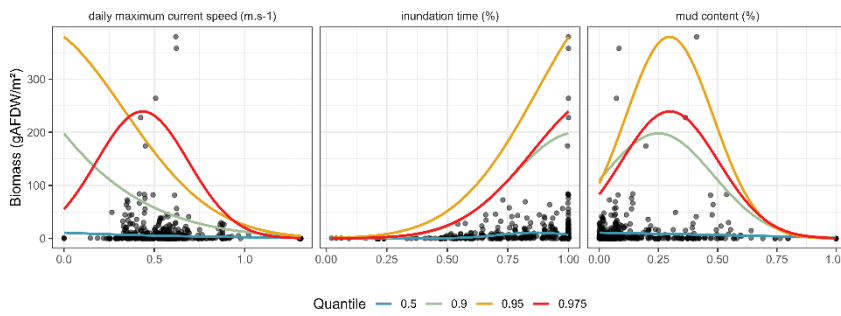
A1



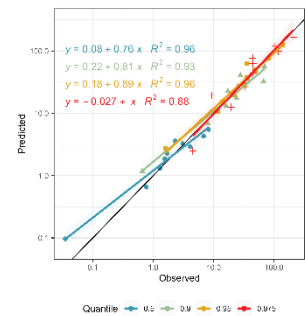
A2



B1



B2



449 Figure 4: First row – (%) Projection on the three abiotic factor axes with observation compared to the
 450 modelled quantiles for the daily maximum current speed (m.s-1), the daily salinity range and the
 451 inundation time (A1). The second column displays the predicted/observed validation plot associated to
 452 this model (A2). Second row – Same figure with the 2nd model with projection on the three abiotic factor
 453 axes: daily maximum current speed (m.s-1), inundation time (%) and mud content (%) (B1); The second
 454 column displays the predicted/observed validation plot associated (B2). Black dots in A1 and B1
 455 represents the observed data; lines the modelled quantiles; Coloured dots in A2 and B2 correspond to
 456 each decile of the modelled distribution and its corresponding observed, black line represents the 1:1
 457 ratio. Quantiles are colour coded as 0.5 in blue, 0.9 in green, 0.95 in orange and 0.975 in red.

$$= A \cdot e^{-\left[\frac{(Predictor1 - \mu1_{\tau})^2}{2 \cdot \sigma1_{\tau}^2} + \frac{(Predictor2 - \mu2_{\tau})^2}{2 \cdot \sigma2_{\tau}^2} + \frac{(Predictor3 - \mu3_{\tau})^2}{2 \cdot \sigma3_{\tau}^2} \right]}$$

458

(1)

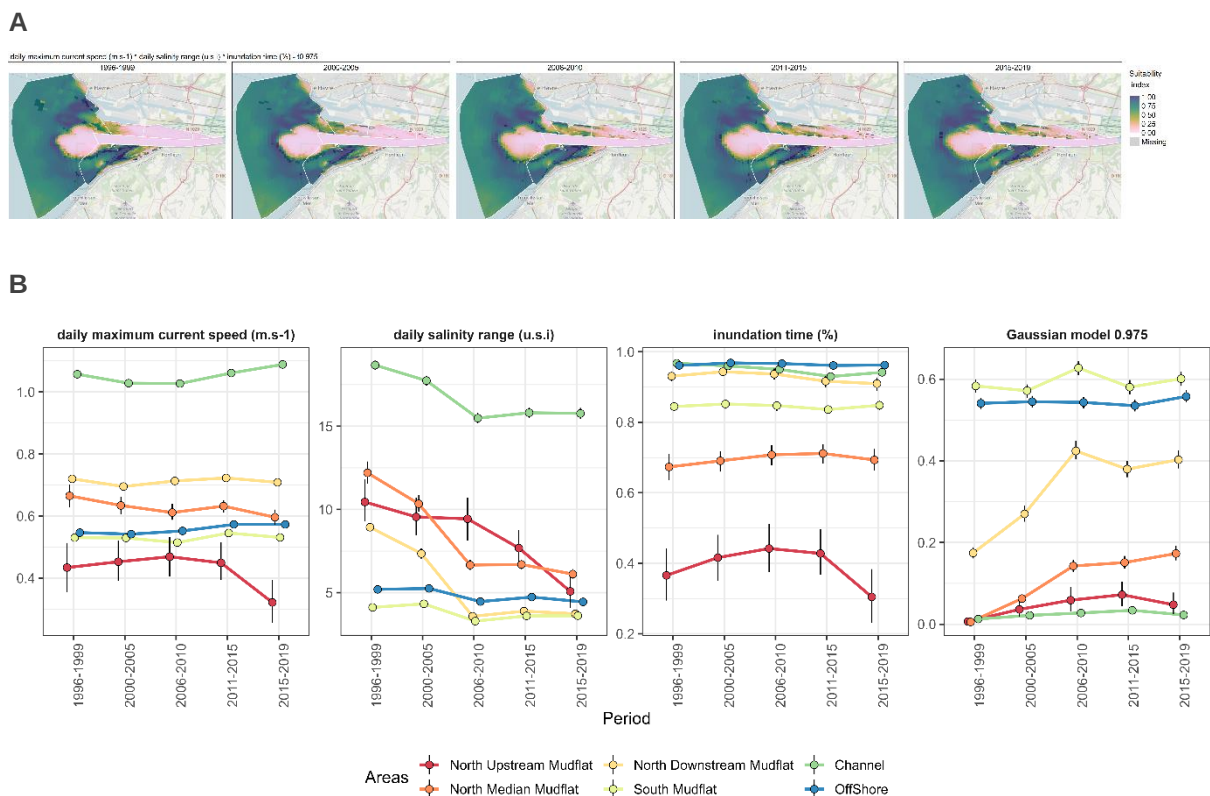
459 Table 4: Coefficient of the models computed with gaussian equation (Equation 1), by quantile and
 460 response.

tau	Biomass (gAFDW/m ²)							Density (ind/m ²)							
	A	μ 1	μ 2	μ 3	σ 1	σ 2	σ 3	A	μ 1	μ 2	μ 3	σ 1	σ 2	σ 3	
daily maximum current speed (m.s-1) * daily salinity range (u.s.i) * inundation time (%)															
0.50	41.55	-2.89	4.26	0.85	1.84	3.51	0.13	9,509.94	-2.24	5.94	0.81	0.93	3.57	0.18	
0.90	716.49	-1.87	1.87	0.97	1.04	5.18	0.22	2,686.24	0.17	4.37	0.95	0.31	4.41	0.21	
0.95	392.63	-0.26	-4.40	1.22	0.58	8.40	0.34	113,728.75	0.39	5.24	3.30	0.24	3.62	0.86	
0.975	3,464.31	0.49	3.27	2.69	0.19	3.79	0.69	421,906.57	0.48	-21.93	2.95	0.19	14.63	0.80	
daily maximum current speed (m.s-1) * inundation time (%) * mud content (%)															
0.50	80.54	-3.06	0.86	-0.28	1.56	0.15	0.71	292.75	0.33	0.79	0.27	0.19	0.17	0.35	
0.90	1,321.22	-1.76	1.03	0.25	0.90	0.26	0.23	7,495.16	0.42	2.26	0.43	0.20	0.86	0.27	
0.95	491.99	-0.17	1.22	0.30	0.50	0.34	0.18	85,227.47	0.46	4.01	0.62	0.20	1.20	0.48	
0.975	272.78	0.43	1.15	0.30	0.25	0.30	0.20	151,774.30	0.50	4.77	0.41	0.21	1.40	0.32	

461 3.4.2 Spatio-temporal variations of habitat suitability

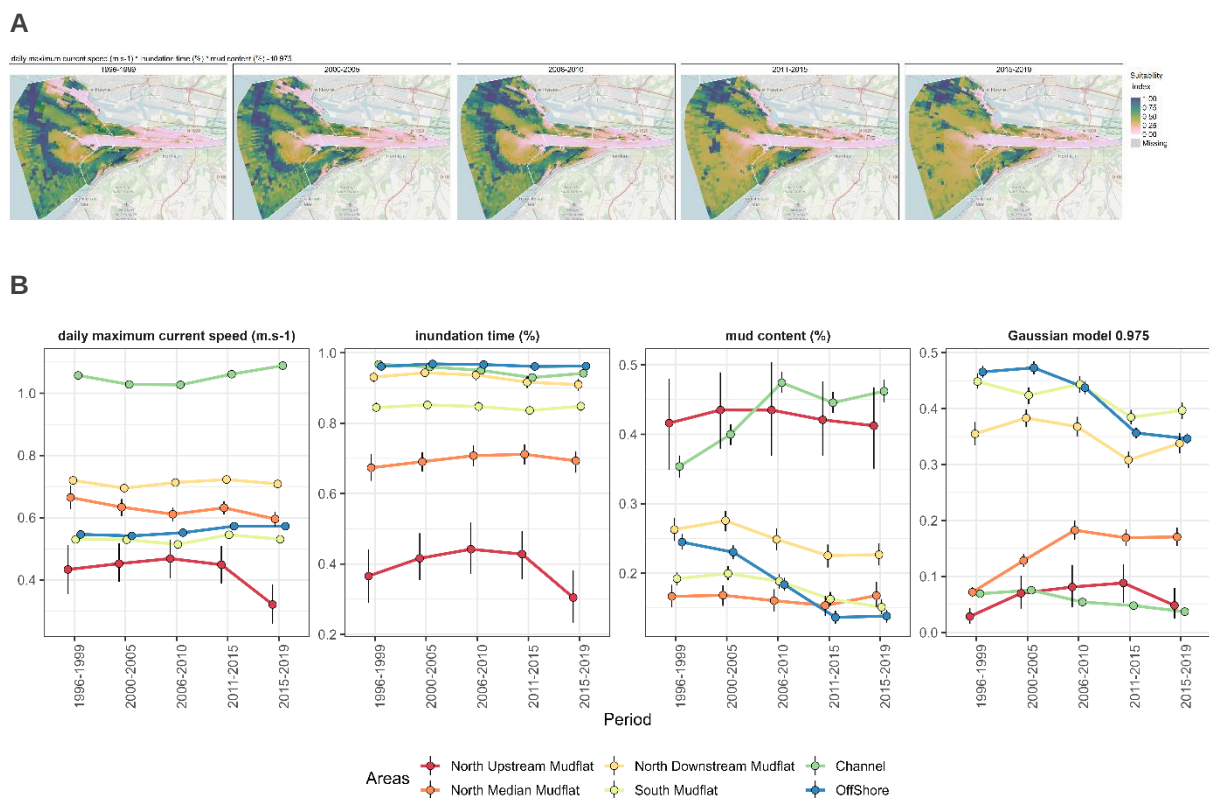
462 The Optimal Ecological Niches, QR ENM with the Gaussian equation, were standardised on the
 463 basis of the model optimum at the 97.5th percentile, to obtain a value ranging from 0, an unfriendly
 464 environment for cockles, to 1, a very suitable environment, which makes it possible to simply assess the
 465 habitability potential of a geographical area. The OEN was applied geographically to define the habitat
 466 suitability of the different areas of the estuary on all periods defined. The suitability index, summary of
 467 the habitat suitability of each period and area is plotted to visualise differences in time and space (density
 468 in Supp. Data 3.4.2).

469 Daily maximum current speed [$m.s^{-1}$] & daily salinity range & inundation time [%]: The maps (Figure
 470 5 A) showed that the channel and northern mudflats were the least favourable areas, the southern
 471 mudflats and offshore were more appropriate, but few locations were really optimum. The suitability
 472 index (Figure 5 B) ranged from 0 to 0.6 and was generally stable, confirming that the most suitable area
 473 was the southern mudflat followed by the offshore zone. The suitability of the northern mudflats
 474 increased after 2005, in particular the northern downstream mudflat. The salinity part of the model had
 475 a noticeable effect on the result of the model, and the increase of habitat suitability for cockles on the 3
 476 northern mudflats can clearly be related to the decrease in the daily salinity range in these sectors.



477 Figure 5: A: Daily maximum current speed [$m.s^{-1}$] & daily salinity range & inundation time [%] model
 478 suitability index applied on the Seine estuary over the five periods. B: Abiotic factors and resulting model
 479 at 97.5th centile suitability index per period and per area for all SDM models with a 95% confidence
 480 interval.

481 Daily maximum current speed [$\text{m}\cdot\text{s}^{-1}$] & inundation time [%] & mud content [%]: The closer to the
 482 mouth of the estuary, the higher the suitability; the offshore area had an advantage, which has
 483 deteriorated since 2011 (Figure 6 A). The apparent patchiness in the habitat suitability in the model
 484 results is linked to the spatial distribution of mud content (Supp data 3.2). The suitability index (Figure 6
 485 B) varies from 0 to 0.5, with the highest value in the offshore area and the lowest in the channel. The
 486 offshore and the southern mudflat were similar in terms of suitability and are the most suitable areas,
 487 joined by the downstream northern mudflat over the last three periods. The northern upstream and
 488 median mudflats showed an increase in habitat suitability over the first three periods from 1996 to 2010.
 489 It is difficult to identify the contribution of one predictor over the others in explaining this trend.



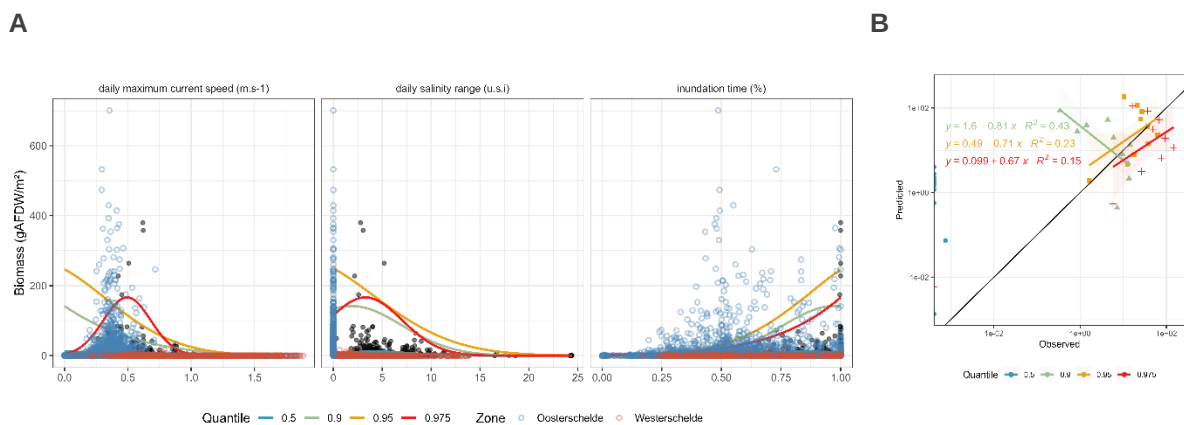
490 *Figure 6: A: Daily maximum current speed [$\text{m}\cdot\text{s}^{-1}$] & inundation time [%] & mud content [%] model*
 491 *suitability index applied on the Seine estuary over the five periods. B: Abiotic factors and resulting model*
 492 *at 97.5th centile suitability index per period and per area for all SDM models with a 95% confidence*
 493 *interval.*

494 3.4.3 Comparison and application to Scheldt basins data

495 The data from the Scheldt estuary was projected onto the Optimal Ecological Niche for the cockle
 496 defined in the Seine estuary using the daily maximum current speed [$\text{m}\cdot\text{s}^{-1}$], daily salinity range and
 497 inundation time [%] model (Figure 7 A). The modelled response in the Scheldt was calculated by
 498 applying this OEN and the performance of the model is shown in Figure 7 B. The model fitted to the
 499 Seine data applied to the Scheldt is not appropriate at the 0.5 quantile, but is better simulated at the
 500 higher quantiles, with positive slopes reaching 0.71 at $\tau=0.95$ and 0.67 at $\tau=0.975$, (Figure 7 B). These

501 regression lines are relatively far from the diagonal, revealing that the model fitted to the Seine data is
 502 not very reliable when applied to the Scheldt basins.

503 When considering the scatterplots of observed biomass as function of the 3 descriptors (Figure 7 A),
 504 we can notice that the response to daily salinity range and the inundation time was different between
 505 the Seine and the Scheldt basins. The distribution of the recorded biomass as a function of the daily
 506 salinity range is difficult to compare, because the present day Oosterschelde basin only receives minor
 507 freshwater inputs, unlike the Westerschelde and thus lacks a full salinity gradient. With regard to
 508 inundation time, there are also discrepancies between the fitted model and the data recorded in the
 509 Scheldt basins, where the best optimal habitat was located on the foreshores with ~50% of the
 510 inundation time, whereas this modelled ENM was predicted at values of 100% of the inundation time.
 511 As for the maximal current speed, the model appeared to be a better fit, but the highest realized cockle's
 512 biomass was observed at a slightly lower current speed (~0.4 m.s⁻¹) even though the difference is within
 513 the error of the numerical model (pers. com. Smolders).



514 *Figure 7: Seine model daily maximum current speed (m.s⁻¹) & daily salinity range & inundation time*
 515 *(%) projection on the three abiotic factor axes with data from Scheldt basins in blue dots for*
 516 *Oosterschelde and red dots for Westerschelde (A) and the predicted/observed validation plot computed*
 517 *on Scheldt application of the model parametrized in the Seine estuary (B). Black dots in A represents*
 518 *the observed data that were used for parameterisation (in the Seine estuary) while green dots are the*
 519 *data from the Scheldt basins; lines represent the model quartiles. Coloured dots in B correspond to each*
 520 *decile of the modelled distribution and its corresponding observed, black line represents the 1:1 ratio.*
 521 *Quantiles are colour coded as 0.5 in blue, 0.9 in green, 0.95 in orange and 0.975 in red.*

522 4 Discussion

523 4.1 Optimal ecological niches for cockles

524 In line with previous knowledge, our study identified current velocity, salinity fluctuations and
 525 inundation time as main environmental drivers of cockle distribution. We can emphasize that the
 526 proposed model which combines the effect of those three factors can be considered valid and robust,
 527 both for biomass and density of cockles, at least in the Seine estuary. This model especially focusses
 528 on the influence of hydrodynamic forcings generated by the tides and the fluvial regime and the
 529 morphology of the estuary, which generates shallow and intertidal areas. Under these conditions, salinity

530 increases with water depth, as it represents the upstream-downstream gradient of the estuary, and the
531 lower the inundation time, the greater the mixing between fresh and marine waters. The optimum given
532 by this model corresponds to low shores (typically the offshore zone with 100% of inundation time),
533 without intense variation in salinity (daily range of ~ 3), in sectors subjected to relatively strong currents
534 ($\sim 0.5 \text{ m.s}^{-1}$). The position on the shore, related to inundation time, must affect the suspension-feeding
535 periods on phytoplankton and also probably the periods when cockles are accessible to predators
536 (Cozzoli et al., 2014). Low inundation time must therefore encourage both survival and growth, mainly
537 related to prey-predator interactions. Regarding the effect of salinity, cockles are often reported to be
538 negatively affected by fresh water supply and salinity rapid shifts are often described as responsible for
539 mass mortality events in cockles, mainly linked to flash floods (Matos et al., 2023). The selection of
540 these predictors agrees well with conclusions of other studies proposing SDM for *Cerastoderma edule*
541 as this was the case in the Scheldt basins, Netherlands (maximal current speed and inundation time –
542 Cozzoli et al., 2014), or the Aveiro lagoon in Portugal (where the predictors contributing the most in the
543 definition of the ENM was salinity, submersion time and current velocity – Matos et al., 2023).
544 Observations in cockle habitats of the British Isles were also in the same direction since the authors
545 mention that cockles were unable to settle in calm waters (Boyden and Russell, 1972) and that the
546 influence of tidal flow was found to be greater than that of salinity, the latter being an indirect indicator
547 of the first and partially redundant.

548 A second alternative model combining the same predictors but with mud content instead of salinity
549 range provide the same level of confidence in terms of robustness of the predictions. We proposed two
550 versions of model to guarantee the best level of transferability and inter-comparison potential with future
551 studies. We must mention, that, to our knowledge, this the first ENM proposed for cockles including mud
552 content. The presence of mud has often been reported to play an important role in cockle performances
553 and spatial distribution. Muddy-sand to sandy-mud sediments are often described as the best optimal
554 habitat for cockles' recruitment and survival, as they provide a perfect balance between oxygenation
555 and microphytobenthos as food supply (Bouma et al., 2001). For instance, in Portuguese lagoons, depth
556 and average sediment grain size were the factors that better explained the probability of species
557 occurrence (Santos et al., 2022). In fact, there must be a relative trade-off between two threatening
558 constraints. On one hand, the absence of mud can clearly be related to strong currents provoking regular
559 mud resuspension in the water column as well as the absence of microphytobenthos as food sources,
560 while, on the other hand, a too intense presence of mud in sediment beds must make increase the
561 vulnerability risks of cockles to eutrophication phenomena (anoxic conditions, contaminant presence).
562 Cockles seem to be able to live in a broad range of habitats with a preference for mixed sediments, and
563 more especially fine sands with a little proportion of mud. The distribution of biomass records across the
564 diversity of sedimentary habitats in the Seine estuary display long distribution tails reaching 0% or 100%
565 of mud content. This result is in agreement with previous observations in other ecosystems. For
566 instance, this bivalve can show a preference for muddy bottoms in Netherland's estuaries, but can also
567 inhabit sediments with a median grain size ranging from 50 μm (fully cohesive) to 250 μm (fully non-
568 cohesive) (Cozzoli et al., 2013). Furthermore, the increase in mud content must also be related to the
569 proximity of river discharge in many ecosystems (with correlation with salinity decrease). This is one

570 reason that we made the choice of one factor or the other in the 2 alternative models. The results are
571 not exactly the same in terms of habitat suitability maps, but both versions generally converge.

572 In a previous study using QR, a SDM for cockles was proposed with only two predictors, the maximal
573 current speed and the inundation time in the Scheldt basins (Cozzoli et al., 2014). They observed that
574 the optimum was found in a medium intertidal zone (~50 % of inundation time) with a maximum current
575 of $\sim 0.5 \text{ m}\cdot\text{s}^{-1}$. So, there is discrepancy between their conclusions and the one of the present study,
576 especially when describing the role played by the inundation time. However, we must mention that, for
577 the dataset of the Scheldt basins, the samples in the subtidal area were discarded because of
578 methodological differences. This choice could explain a part of the contrasting conclusions, since we
579 can have doubts if subtidal zones are really not occupied by cockle populations in the Scheldt basins. It
580 is also possible that because of contrasting conditions (slope of the cross-shore, hydrodynamic
581 conditions or morphological landscapes...), the settlement preference can occur either at the minimum
582 limit of the intertidal shore as observed in the Seine or in the middle position of intertidal shores, as
583 observed in the Scheldt basins. This is unlikely that these contrasting preferences derive from genetic
584 differences between populations, since studies investigating the genetic patterns of cockles in Europe
585 suggest a common genetic sub-population with a northern group globally consisting of the northern
586 North Sea (Vera et al., 2023). These contrasting findings must rather be related to historical processes
587 and local adaptation of cockle populations, despite the high level of larval connectivity across northern
588 North Sea.

589 In another study located at the Ria of Aveiro in Portugal, the optimal habitat was observed for calmer
590 conditions ($\sim 0.2 \text{ m}\cdot\text{s}^{-1}$) compared to our results, but the most suitable habitat was found in similar
591 conditions to our results regarding inundation time and salinity, since they found increasingly suitable
592 conditions with the increase of salinity and submersion time (optimum for subtidal and marine waters).
593 So, there could be a shift in current velocity and submersion time in the definition of the most suitable
594 habitat, depending on the ecosystem. Even if, this time, genetic diversity can partly explain some
595 biological differences (Vera et al., 2023), since the genetic structure of cockles is clearly different
596 between South Portugal and North Sea areas, we can suppose that the biological response to tidal
597 currents can be relatively broad for cockles, generally, and could shift depending on the local
598 environment. Apparently, cockles do not like still water at all in any ecosystem, and they clearly prefer
599 locations with dynamic waters everywhere. Globally, there is a general consensus that cockles
600 appreciate habitats located between the lower limit of the intertidal-subtidal shores and mid-shore
601 positions, but cockles can prefer either the lower limit between intertidal and subtidal zones (as in the
602 Seine estuary), while they can prefer the central intertidal shores in other places as in the Scheldt basins.

603 A more detailed analysis of the contrasting conditions between the Westerschelde, Oosterschelde
604 and Seine basins reveals obvious divergences that preclude the definition of a generic optimum for
605 cockles, reliable everywhere. In particular, the Oosterschelde is a virtually closed basin with little
606 freshwater input, whereas the Seine and the Oosterschelde are open estuaries. These discrepancies
607 clearly indicate that the optimal conditions for cockles are indeed different in the three basins, and
608 especially in the Oosterschelde. These conditions lead to different covariance structures for the physical

609 factors, but do not call the model into question, although not all conditions present in the Oosterschelde
610 are represented in the Seine data. The upper boundary models cannot really extrapolate to new
611 conditions, but they can be successfully applied to new scenarios under the boundary conditions of the
612 training data set. In general, the Oosterschelde, which is not influenced by freshwater input and has
613 calmer waters, represents the best optimal habitat in this system, unlike the Seine or the Oosterschelde.

614 Questions can also be raised about the number of predictors to be retained in the ENM for cockles
615 and the level of complexity to be retained. First, it is possible that among the three predictors of the two
616 models we propose, there is one that contributes less and could be removed, or that does not shed light
617 because of its redundancy with another more structuring factor. By testing the fit of the QR models with
618 different combinations of predictors, the results were clearly less well predicted with only two descriptors.
619 Of all the physical factors, we are relatively confident in the selection of the predictors we decided to
620 retain, namely maximum current velocity, inundation time and a third predictor (either salinity or silt
621 content).

622 It seems unlikely that the addition of descriptors extractable from hydrodynamic 3D model could bring
623 improvements, in terms of validation or model quality. However, the role of food availability and
624 especially the chlorophyll concentration in the seawater must be relevant for these suspension-feeders.
625 For instance, the study in the Ria of Aveiro (Matos et al., 2023) retained chl a concentration as well as
626 nitrate concentration as secondary predictors. In the Wadden sea (Netherlands), the residual of a SDM
627 show some correlation level with chl a concentration, suggesting a potential improvement by adding this
628 predictor (Folmer et al., 2017). In Baie des Veys, in Normandy (France), a study focused on the coupling
629 between benthic and pelagic components had also identified that the best correlated variable to cockle
630 biomass was the pelagic chl a concentration even if this chl a was more related to resuspended
631 microphytobenthos to phytoplankton in this case (Ubertini et al., 2012). The abundance of
632 microphytobenthic biofilms, especially high in sand-mud mixtures (Morelle et al., 2020) and their
633 resuspension rates must be very relevant as a food supply for cockles (Rakotomalala et al., 2015;
634 Sauriau and Kang, 2000; Ubertini et al., 2012). This addition of chl a concentration and trophic predictor
635 could be modelled by incorporating a biogeochemical model coupled to a 3D hydro-sedimentary model.
636 Unfortunately, this kind of biogeochemical models are not so easily available everywhere. In an attempt
637 of exploring a ENM that could be transferred to other systems, it seems essential to consider food
638 limitation and carrying capacities of the ecosystems in terms of phytoplankton or microphytobenthos.
639 Herman et al. (1999) clearly showed a dependence of system-averaged benthic biomass on the
640 magnitude of the spring phytoplankton bloom and there is a clear dependence of macrozoobenthic
641 biomass and especially that of suspension-feeders on primary production rate when comparing different
642 ecosystems. For instance, the fact that cockles biomass is very low in the Westerschelde compared to
643 the Oosterschelde, can be clearly explained by the primary production level that can exceed $\sim 300 \text{ gC.m}^{-2}.\text{y}^{-1}$
644 in the Oosterschelde, with a factor of 3 higher than in the Westerschelde (Herman et al., 1999). In
645 the Seine estuary, the recent estimate of primary production provides the value of $65 \text{ gC.m}^{-2}.\text{y}^{-1}$ (Morelle
646 et al., 2018). There is also a possibility to improve predictions of ENM of benthic bivalves by including
647 other biotic variables, as observed in New Zealand where the inclusion of co-occurring species improves
648 the prediction quality by integrating ecological theory about species interaction (Stephenson et al.,

649 2022). However, increasing the level of complexity too much is not necessarily a model improvement,
650 since there a lot of redundancy and correlation among variables, when adding several predictors that
651 could interplay.

652 4.2 Assessment of the methodology

653 The construction of an ENM using QR makes it possible to define an OEN, i.e. the optimal biological
654 development in a given ecosystem. This involves defining the environmental conditions for which the
655 highest biomass is possible according to a defined set of factors. This approach differs from an AM
656 approach, where the maximum number of available factors is used to define a species distribution
657 model. Simplifying the environment to a limited number of factors makes it easier to apply and transfer
658 the niche to other environments, allowing comparisons between different locations. QR models could
659 not only be used to detect heterogeneous effects of descriptors at different quantiles of the biological
660 response, but also offer more robust and comprehensive estimates compared to mean regression, when
661 the normality assumption is violated or if there are outliers or long tails of the distribution. These
662 advantages make QR attractive, particularly if they are extended to apply independent datasets (Huang
663 et al., 2017).

664 By comparing the recorded data with the niche modelling, it is possible to assess its biological and
665 physiological relevance. We chose to use a Gaussian equation to rigorously link the biological response
666 to abiotic factors, based on current knowledge and classical distribution law reliable for biological
667 populations in response to any environmental factor. This type of equation has the advantage of
668 obtaining a unimodal response, unlike what can be obtained with a B-spline at the third degree, for
669 example. This choice avoids retaining a model that seems quite good in terms of adjustments, but which
670 simulates unfounded distributions. In addition, the niche model thus obtained is a continuous response,
671 i.e. with no tipping point towards an unfavourable state, the biological reality of which is debatable when
672 the selected factors are considered, in an estuarine environment defined by gradients and strong
673 variations in abiotic conditions.

674 On the other hand, the QR approach makes it possible to respond to the very local effects and natural
675 patchiness that can affect biological populations and lead to very high densities of a species in a local
676 'patch', a phenomenon often observed in estuarine environments. Community self-organisation takes
677 place at several overlapping spatial scales, strongly expressed by tidal constraints, where micro-scale
678 organisations are able to create micro-climates that can accommodate very high densities of fauna
679 (Ettema and Wardle, 2002; Le Hir and Hily, 2005; Thrush et al., 2005; Underwood and Chapman, 1996).
680 The aim of this study was to define the HMS conditions most favourable to the development of a species,
681 and not necessarily the niche representing the most exceptional circumstances, hence the choice of a
682 high but not necessarily maximum quantile. The very high quantiles correspond to the niche that reflects
683 the biological observations resulting from the patchy distribution of species. Species distributions and
684 the inherent patchiness can be studied in details on the basis of the maximum density of intertidal
685 species, for instance (Thrush et al., 2003).

686 Whatever the model used, the quality of a SDM depends first and foremost on the reliability of the
687 input data. The Seine biological data used in this study comes from community monitoring programmes
688 with a continuity of practices, and even of operators, which makes it possible to process data together
689 over such a long period of time. The succession of generations in a population in an evolving ecosystem
690 is key information for understanding the dynamics of a population in its environment. With regard to
691 environmental data, the abiotic field data, synchronous with the biological data, are susceptible to
692 highlight very small atypical habitats rather than macro-spatial trends. The use of a hydro-morpho-
693 sedimentary model therefore makes it possible to better describe the overall “smoothed” environment,
694 with a large scale.

695 However, the synthesis of abiotic data, which is generally available at much higher frequencies than
696 biological data, is subject to choices that have an impact on the way in which the niche is interpreted. In
697 this study, the abiotic data are summarised at their annual median (over a hydrological year, from
698 October to September) and aligned with the biological samples, so that they represent the recent history
699 of the individual sampled. The long time series (at least 2 decades) then makes it possible to represent
700 an ecosystem in which we find a fauna that is subject to this local climate, which may or may not evolve
701 over generations.

702 In intertidal environments, the interactions between an environment and its biotope are part of a
703 feedback loop: organisms are adapted to certain abiotic conditions, but they are able to significantly
704 modify certain key abiotic parameters that define their environment, in particular sediment erosion
705 parameters via bioturbation (Kristensen et al., 2012). Cockles, for example, are known eco-engineers
706 that can modify their environment, in particular sediment content (Donadi et al., 2014, 2013). They
707 modify their habitat to obtain better conditions (Li et al., 2017) and interact strongly with the
708 microphytobenthos, creating biofilms that modify the erodibility of the sediments (Eriksson et al., 2017;
709 Ubertini et al., 2012). These bioturbation processes are not yet included in HMS models, even though
710 they can have a significant impact on estuary morphology (Orvain et al., 2012). Including these biota-
711 mediated erodibility factors in HMS models may therefore have mitigating effects on the long-term
712 evolution of habitats (Lehuen et al., 2024), and this should significantly improve the prediction of abiotic
713 factors and their use for defining ENM/SDM. The aim is to better integrate the local effects exerted by
714 benthic fauna (in particular bioturbation) into complex large-scale interactions in order to consolidate
715 long-term projections.

716 Moreover, the ENM obtained applied in SDM is not capable of predicting a drastic change in
717 population that would be subject to short episodes of stressful events. In particular, constraining
718 episodes occurring in the context of climate change could become a threat to the future of a population,
719 leading to drastic changes in community succession initiated by a long-term change in physical
720 conditions (Baltar et al., 2019). Examples include heat waves or highly erosive storms, the duration,
721 intensity and frequency of which can affect the recruitment and development of populations. This is
722 where the long-term climate approach comes up against its real limit: the representativeness of climate
723 variability and the question of event frequency, which is the key to understanding the effects of climate
724 change that could lead to a shock to biodiversity or productivity. Extreme events are insufficiently defined

725 by a simple maximum of environmental values, as this has been demonstrated experimentally for the
726 case of heat waves (Zhou et al., 2022).

727 Abiotic data from HMS models can be used to describe complex patterns between the main physical
728 factors, but the evolution of ecosystems in response to climate change may lead to previously
729 unconsidered parameters becoming critical parameters for biological development, such as pH. Indeed,
730 the acidification of marine waters is an identified consequence of their warming, and its impact on
731 bivalves' organisms has been demonstrated (Thomas and Bacher, 2018). There are experimental
732 studies on the biological response to ranges of variation in temperature, salinity or pH, which can provide
733 a better understanding of the mechanistic basis of metabolisms on organism performance (Hale et al.,
734 2011; Łapucki and Normant, 2008; Lemasson et al., 2017; Madeira et al., 2021; Medeiros et al., 2020;
735 Ong et al., 2017; Peteiro et al., 2018). However, in environments such as the Seine estuary, pH is not
736 traditionally considered to be an environmental factor that plays an important role in the distribution of
737 species at least during the past survey planning.

738 Taken together, all these limitations justify recommending a cautious interpretation of the use of niche
739 models in extrapolative and long-term projections. Indeed, by defining an average trend in the evolution
740 of HMS factors in the estuary in order to assess the future of a species, this exercise could completely
741 miss the dangers encountered by the population studied and provide erroneous information, whether
742 reassuring or alarming.

743 4.3 A tool for ecosystem management

744 ENMs and their SDM application are tools that can effectively be used for the management of natural
745 areas, highlighting the spatio-temporal differences in a given territory according to selected factors. In
746 this case, the model can be used to monitor the potential productivity of target species, to ensure that
747 the presence of a population that provides the ecosystem services required by the estuary is facilitated.
748 ENM/SDM can also be used to monitor the progress of an invasive species in a territory (Srivastava et
749 al., 2019), measure the impact of anthropogenic structures (Cozzoli et al., 2017), or define a
750 conservation strategy for an endangered species (Frans et al., 2022).

751 The use of an ENM in a given space depends on the technique used. Existing SDMs using the AM
752 approach provide high-performance SDMs, but it is not possible to apply them to the data set available
753 to us. This led us to choose the QR ENM method, which provides a set of equations based on a
754 reasonable number of factors that are generally accessible in the context of managing an ecosystem
755 such as an estuary.

756 As seen in the previous paragraphs, the ENM obtained and its application in SDM makes it possible
757 to control a geographical area such as an estuary in the medium term (~10 years). However, in this
758 study we would rather not project the niche into a future environment to avoid any speculation, as it
759 would probably not be able to respond to distant horizons for which the environment would be more
760 significantly modified. The tool nevertheless remains operational in a context of management of a natural
761 area subject to anthropogenic pressure, simply illustrating the zones favourable to the cockles. The

762 habitat suitability model also makes it possible to identify any drift in the areas of interest, and to begin
763 a diagnosis of the causes of this drift, by adapting the temporal and spatial resolution as required. In
764 fact, as the SDMs are linked to the HMS variables, the habitat suitability is a good indicator of the
765 potential levers for dealing with changes in ecosystems, in particular due to human activities, as well as
766 the effects of global climate change.

767 The results of this study showed, for example, an improvement in the habitability of cockles on the
768 intertidal mudflats of the Seine, due to the saline intrusion already obvious. This trend should continue
769 in the future for cockle, but at the expense of the more euryhaline species that typically colonise intertidal
770 mudflats further upstream, such as *Hediste diversicolor* or *Scrobicularia plana*. However, increasing
771 salinity can be accompanied by a reduction in freshwater input, which can lead to a limitation in nutritive
772 salts and therefore in primary and secondary productivity, resulting in a risk of population declines and
773 a global rarefaction of benthic communities, whatever the niche.

774 The ENM/SDM are generally developed for an isolated species, but the management of a natural
775 area requires an approach not only on a broad spatio-temporal scale, but also on the scale of species
776 communities and the ecosystem services that we wish to maintain. The biodiversity approach using the
777 Shannon index has been used in an SDM (Cozzoli et al., 2017). In another way, the introduction of inter-
778 species interactions has been explored in the form of an explanatory biological factor in an SDM
779 (Stephenson et al., 2022), which improves the model but reveals complex interaction patterns as soon
780 as two species are studied. In addition, we can envisage modelling the biological response of a species
781 community according to a set of environmental variables, in order to represent the complete biotic
782 environment, as initiated in the Wadden Sea (Folmer et al., 2017). However, defining a community of
783 species is very closely linked to the analysis prism chosen. Depending on the question raised, it will be
784 relevant to construct a community according to life traits, functional traits - trophic, bioengineering -, the
785 food web or the ecosystem services that the macrofauna can provide.

786 5 Conclusion

787 Because of their complex structure and strong gradients, understanding estuarine ecosystems can
788 benefit from modelling the ecological niches of its fauna using ENM and SDM tools. The extraction of
789 physical descriptors from 3D HMS models of water and sediment transport and the method of describing
790 ecological niches using quantile regression enabled a detailed analysis of the environmental needs of
791 the cockle. The two models built in this study, QR ENM at the 97.5th percentile with a Gaussian equation,
792 combining maximum daily current speed, inundation time and daily salinity range or mud content as a
793 third predictive factor, provide a robust description of the cockle's optimal ecological niche. This niche,
794 standardised in the form of habitat suitability, allowed a geographical visualisation of the habitability of
795 the estuary for the cockle, as well as its temporal evolution by areas of interest. The application of one
796 of the ENMs obtained to another estuary showed the potential for transferability, while revealing the
797 need to define a niche with additional elements. In particular, it seems necessary to integrate trophic
798 components and in particular the availability of microalgal resources (phytoplankton and
799 microphytobenthos). Based on general theories concerning the relationship between primary and

800 secondary productivity, it seems relevant to incorporate a model simulating chl a into 3D models before
801 being able to propose a truly generic and transferable ENM model. This could be debated, since the
802 representation of the correlation between drivers (including food) could make the difference.

803 Acknowledgements

804 The authors thank Tjeerd Bouma for his guidance and insight on the MELTING POTES project; Brian
805 Cade for his precious help on quantile regression; The GIP Seine Aval, the Maison de l'Estuaire, the
806 Cellule du Suivi du Littoral Normand and the Grand Port Maritime du Havre for the biological datasets;
807 IFREMER for the Mars3D model dataset. The authors acknowledge anonymous reviewers for their
808 valuable comments and suggestions.

809 Funding

810 This research was supported by the *Region Normandie* (A. Lehuen's PhD) and by the *Office Français*
811 *pour la Biodiversité* (the MELTING POTES project).

812 CRediT author statement

813 A. Lehuen: Conceptualization, Methodology, Formal analysis, Writing - Original Draft, Funding
814 acquisition ; C. Dancie: Resources, Data Curation, Writing - Review & Editing ; F. Grasso: Resources,
815 Data Curation, Writing - Review & Editing; F. Orvain: Conceptualization, Methodology, Validation,
816 Resources, Writing - Review & Editing, Supervision, Project administration, Funding acquisition

817 References

- 818 Akaike, H., 1974. A new look at the statistical model identification. *IEEE Trans. Autom. Control* 19, 716–
819 723. <https://doi.org/10.1109/TAC.1974.1100705>
- 820 Anderson, M.J., 2008. Animal-sediment relationships re-visited: Characterising species' distributions
821 along an environmental gradient using canonical analysis and quantile regression splines. *J.*
822 *Exp. Mar. Biol. Ecol.* 366, 16–27. <https://doi.org/10.1016/j.jembe.2008.07.006>
- 823 Arlinghaus, P., Zhang, W., Wrede, A., Schrum, C., Neumann, A., 2021. Impact of benthos on
824 morphodynamics from a modeling perspective. *Earth-Sci. Rev.* 221, 103803.
825 <https://doi.org/10.1016/j.earscirev.2021.103803>
- 826 Aulert, C., Provost, P., Bessineton, C., Dutilleul, C., 2009. Les mesures compensatoires et
827 d'accompagnement Port 2000 : retour d'expériences. *Ingénieries* 55–72.

828 Austin, M., 2007. Species distribution models and ecological theory: A critical assessment and some
829 possible new approaches. *Ecol. Model.* 200, 1–19.
830 <https://doi.org/10.1016/j.ecolmodel.2006.07.005>

831 Austin, M.P., 2002. Spatial prediction of species distribution: an interface between ecological theory and
832 statistical modelling. *Ecol. Model.* 157, 101–118. [https://doi.org/10.1016/S0304-3800\(02\)00205-3](https://doi.org/10.1016/S0304-3800(02)00205-3)

834 Bacouillard, L., Baux, N., Dauvin, J.-C., Desroy, N., Geiger, K.J., Gentil, F., Thiébaud, É., 2020. Long-
835 term spatio-temporal changes of the muddy fine sand benthic community of the Bay of Seine
836 (eastern English Channel). *Mar. Environ. Res.* 161, 105062.
837 <https://doi.org/10.1016/j.marenvres.2020.105062>

838 Baffreau, A., Pezy, J.-P., Dancie, C., Chouquet, B., Hacquebart, P., Poisson, E., Foveau, A., Joncourt,
839 Y., Duhamel, S., Navon, M., Marmin, S., Dauvin, J.-C., 2017. Mapping benthic communities: An
840 indispensable tool for the preservation and management of the eco-socio-system in the Bay of
841 Seine. *Reg. Stud. Mar. Sci.* 9, 162–173. <https://doi.org/10.1016/j.rsma.2016.12.005>

842 Baltar, F., Bayer, B., Bednarsek, N., Deppeler, S., Escribano, R., Gonzalez, C.E., Hansman, R.L.,
843 Mishra, R.K., Moran, M.A., Repeta, D.J., Robinson, C., Sintes, E., Tamburini, C., Valentin, L.E.,
844 Herndl, G.J., 2019. Towards Integrating Evolution, Metabolism, and Climate Change Studies of
845 Marine Ecosystems. *Trends Ecol. Evol.* 34, 1022–1033.
846 <https://doi.org/10.1016/j.tree.2019.07.003>

847 Beck, M.W., Heck, K.L., Able, K.W., Childers, D.L., Eggleston, D.B., Gillanders, B.M., Halpern, B., Hays,
848 C.G., Hoshino, K., Minello, T.J., Orth, R.J., Sheridan, P.F., Weinstein, M.P., 2001. The
849 Identification, Conservation, and Management of Estuarine and Marine Nurseries for Fish and
850 Invertebrates. *BioScience* 51, 633. [https://doi.org/10.1641/0006-3568\(2001\)051\[0633:TICAMO\]2.0.CO;2](https://doi.org/10.1641/0006-3568(2001)051[0633:TICAMO]2.0.CO;2)

852 Boesch, D.F., Turner, R.E., 1984. Dependence of fishery species on salt marshes: The role of food and
853 refuge. *Estuaries* 7, 460–468. <https://doi.org/10.2307/1351627>

854 Bouma, H., Duiker, J.M.C., de Vries, P.P., Herman, P.M.J., Wolff, W.J., 2001. Spatial pattern of early
855 recruitment of *Macoma balthica* (L.) and *Cerastoderma edule* (L.) in relation to sediment
856 dynamics on a highly dynamic intertidal sand flat. *J. Sea Res.* 15.

857 Boyden, C.R., Russell, P.J.C., 1972. The Distribution and Habitat Range of the Brackish Water Cockle
858 (*Cardium* (*Cerastoderma*) *glaucum*) in the British Isles. *J. Anim. Ecol.* 41, 719.
859 <https://doi.org/10.2307/3205>

860 Brown, J.H., Stevens, G.C., Kaufman, D.M., 1996. The Geographic Range: Size, Shape, Boundaries,
861 and Internal Structure. *Annu. Rev. Ecol. Syst.* 27, 597–623. <https://doi.org/10.2307/2097247>

862 Cade, B.S., Noon, B.R., 2003. A gentle introduction to quantile regression for ecologists. *Front. Ecol.*
863 *Environ.* 1, 412–420. [https://doi.org/10.1890/1540-9295\(2003\)001\[0412:AGITQR\]2.0.CO;2](https://doi.org/10.1890/1540-9295(2003)001[0412:AGITQR]2.0.CO;2)

864 Cade, B.S., Noon, B.R., Flather, C.H., 2005. Quantile regression reveals hidden bias and uncertainty in
865 habitat models. *Ecology* 86, 786–800. <https://doi.org/10.1890/04-0785>

866 Cade, B.S., Terrell, J.W., Schroeder, R.L., 1999. Estimating effects of limiting factors with regression
867 quantiles 80, 13.

868 Carss, D.N., Brito, A.C., Chainho, P., Ciutat, A., de Montaudouin, X., Fernández Otero, R.M., Filgueira,
869 M.I., Garbutt, A., Goedknecht, M.A., Lynch, S.A., Mahony, K.E., Maire, O., Malham, S.K., Orvain,
870 F., van der Schatte Olivier, A., Jones, L., 2020. Ecosystem services provided by a non-cultured
871 shellfish species: The common cockle *Cerastoderma edule*. *Mar. Environ. Res.* 158, 104931.
872 <https://doi.org/10.1016/j.marenvres.2020.104931>

873 Chapman, M., Tolhurst, T., Murphy, R., Underwood, A., 2010. Complex and inconsistent patterns of
874 variation in benthos, micro-algae and sediment over multiple spatial scales. *Mar. Ecol. Prog.*
875 *Ser.* 398, 33–47. <https://doi.org/10.3354/meps08328>

876 Cozzoli, F., Bouma, T., Ysebaert, T., Herman, P.M.J., 2013. Application of non-linear quantile regression
877 to macrozoobenthic species distribution modelling: comparing two contrasting basins. *Mar.*
878 *Ecol. Prog. Ser.* 475, 119–133. <https://doi.org/10.3354/meps10112>

879 Cozzoli, F., Eelkema, M., Bouma, T.J., Ysebaert, T., Escaravage, V., Herman, P.M.J., 2014. A Mixed
880 Modeling Approach to Predict the Effect of Environmental Modification on Species Distributions.
881 *PLoS ONE* 9, e89131. <https://doi.org/10.1371/journal.pone.0089131>

882 Cozzoli, F., Smolders, S., Eelkema, M., Ysebaert, T., Escaravage, V., Temmerman, S., Meire, P.,
883 Herman, P.M.J., Bouma, T.J., 2017. A modeling approach to assess coastal management
884 effects on benthic habitat quality: A case study on coastal defense and navigability. *Estuar.*
885 *Coast. Shelf Sci.* 184, 67–82. <https://doi.org/10.1016/j.ecss.2016.10.043>

886 Crossland, C.J., Baird, D., Ducrotoy, J.-P., Lindeboom, H., Buddemeier, R.W., Dennison, W.C.,
887 Maxwell, B.A., Smith, S.V., Swaney, D.P., 2005. The Coastal Zone — a Domain of Global
888 Interactions, in: Crossland, C.J., Kremer, H.H., Lindeboom, H.J., Marshall Crossland, J.I., Le
889 Tissier, M.D.A. (Eds.), *Coastal Fluxes in the Anthropocene*, *Global Change — The IGBP Series*.
890 Springer Berlin Heidelberg, Berlin, Heidelberg, pp. 1–37. [https://doi.org/10.1007/3-540-27851-](https://doi.org/10.1007/3-540-27851-6_1)
891 [6_1](https://doi.org/10.1007/3-540-27851-6_1)

892 Dauvin, J.-C., 2015. History of benthic research in the English Channel: From general patterns of
893 communities to habitat mosaic description. *J. Sea Res.*, *MeshAtlantic: Mapping Atlantic Area*
894 *Seabed Habitats for Better Marine Management* 100, 32–45.
895 <https://doi.org/10.1016/j.seares.2014.11.005>

896 Dauvin, J.C., Ruellet, T., Desroy, N., Janson, A.-L., 2006. Indicateurs benthiques de l'état des
897 peuplements benthiques de l'estuaire marin et moyen et de la partie orientale de la Baie de
898 Seine. *Rapport scientifique Seine-Aval* 3. Theme 3: Tableau de bord et indicateurs
899 opérationnels. GIP Seine Aval.

- 900 Degraer, S., Verfaillie, E., Willems, W., Adriaens, E., Vincx, M., Van Lancker, V., 2008. Habitat suitability
901 modelling as a mapping tool for macrobenthic communities: An example from the Belgian part
902 of the North Sea. *Cont. Shelf Res.* 28, 369–379. <https://doi.org/10.1016/j.csr.2007.09.001>
- 903 Donadi, S., van der Zee, E.M., van der Heide, T., Weerman, E.J., Piersma, T., van de Koppel, J., Olf, H.,
904 Bartelds, M., van Gerwen, I., Eriksson, B.K., 2014. The bivalve loop: Intra-specific facilitation
905 in burrowing cockles through habitat modification. *J. Exp. Mar. Biol. Ecol.* 461, 44–52.
906 <https://doi.org/10.1016/j.jembe.2014.07.019>
- 907 Donadi, S., Westra, J., Weerman, E.J., van der Heide, T., van der Zee, E.M., van de Koppel, J., Olf, H.,
908 Piersma, T., van der Veer, H.W., Eriksson, B.K., 2013. Non-trophic Interactions Control Benthic
909 Producers on Intertidal Flats. *Ecosystems* 16, 1325–1335. [https://doi.org/10.1007/s10021-013-](https://doi.org/10.1007/s10021-013-9686-8)
910 9686-8
- 911 Elith, J., Leathwick, J.R., 2009. Species Distribution Models: Ecological Explanation and Prediction
912 Across Space and Time. *Annu. Rev. Ecol. Evol. Syst.* 40, 677–697.
913 <https://doi.org/10.1146/annurev.ecolsys.110308.120159>
- 914 Eriksson, B.K., Westra, J., van Gerwen, I., Weerman, E., van der Zee, E., van der Heide, T., van de
915 Koppel, J., Olf, H., Piersma, T., Donadi, S., 2017. Facilitation by ecosystem engineers
916 enhances nutrient effects in an intertidal system. *Ecosphere* 8, e02051.
917 <https://doi.org/10.1002/ecs2.2051>
- 918 Ettema, C.H., Wardle, D.A., 2002. Spatial soil ecology. *Trends Ecol. Evol.* 17, 177–183.
919 [https://doi.org/10.1016/S0169-5347\(02\)02496-5](https://doi.org/10.1016/S0169-5347(02)02496-5)
- 920 Folmer, E., Dekinga, A., Holthuijsen, S., 2017. Species Distribution Models of Intertidal Benthos - Tools
921 for Assessing the Impact of Physical and Morphological Drivers on Benthos and Birds in the
922 Wadden Sea. NIOZ Royal Netherlands Institute for Sea Research, Texel.
- 923 Franklin, J., 2010. Mapping Species Distributions: Spatial Inference and Prediction, Ecology,
924 Biodiversity and Conservation. Cambridge University Press, Cambridge.
925 <https://doi.org/10.1017/CBO9780511810602>
- 926 Frans, V.F., Augé, A.A., Fyfe, J., Zhang, Y., McNally, N., Edelhoff, H., Balkenhol, N., Engler, J.O., 2022.
927 Integrated SDM database: Enhancing the relevance and utility of species distribution models in
928 conservation management. *Methods Ecol. Evol.* 13, 243–261. [https://doi.org/10.1111/2041-](https://doi.org/10.1111/2041-210X.13736)
929 210X.13736
- 930 Goberville, E., Beaugrand, G., Sautour, B., Tréguer, P., Somlit, T., 2010. Climate-driven changes in
931 coastal marine systems of western Europe. *Mar. Ecol. Prog. Ser.* 408, 129–147.
932 <https://doi.org/10.3354/meps08564>
- 933 Gosling, E.M., 2003. Bivalve molluscs: biology, ecology, and culture, Fishing News Books. ed. Blackwell
934 Publishing, Oxford ; Malden, MA.
- 935 Grassle, F.J., 2013. Marine Ecosystems, in: Encyclopedia of Biodiversity. Elsevier, pp. 45–55.
936 <https://doi.org/10.1016/B978-0-12-384719-5.00290-2>

- 937 Grasso, F., Bismuth, E., Verney, R., 2021. Unraveling the impacts of meteorological and anthropogenic
938 changes on sediment fluxes along an estuary-sea continuum. *Sci. Rep.* 11, 20230.
939 <https://doi.org/10.1038/s41598-021-99502-7>
- 940 Grasso, F., Bismuth, E., Verney, R., 2019. ARES hindcast [WWW Document]. *Sextant*. URL
941 <https://sextant.ifremer.fr/geonetwork/srv/api/records/8f5ec053-52c8-4120-b031-4e4b6168ff29>
942 (accessed 5.13.23).
- 943 Grasso, F., Le Hir, P., 2019. Influence of morphological changes on suspended sediment dynamics in
944 a macrotidal estuary: diachronic analysis in the Seine Estuary (France) from 1960 to 2010.
945 *Ocean Dyn.* 69, 83–100. <https://doi.org/10.1007/s10236-018-1233-x>
- 946 Grasso, F., Verney, R., Le Hir, P., Thouvenin, B., Schulz, E., Kervella, Y., Khojasteh Pour Fard, I.,
947 Lemoine, J.-P., Dumas, F., Garnier, V., 2018. Suspended Sediment Dynamics in the Macrotidal
948 Seine Estuary (France): 1. Numerical Modeling of Turbidity Maximum Dynamics. *J. Geophys.*
949 *Res. Oceans* 123, 558–577. <https://doi.org/10.1002/2017JC013185>
- 950 Guarini, J., Blanchard, G., Bacher, C., Gros, P., Riera, P., Richard, P., Gouleau, D., Galois, R., Prou, J.,
951 Sauriau, P., 1998. Dynamics of spatial patterns of microphytobenthic biomass: inferences from
952 a geostatistical analysis of two comprehensive surveys in Marennes-Oléron Bay (France). *Mar.*
953 *Ecol. Prog. Ser.* 166, 131–141. <https://doi.org/10.3354/meps166131>
- 954 Guisan, A., Thuiller, W., 2005. Predicting species distribution: offering more than simple habitat models.
955 *Ecol. Lett.* 8, 993–1009. <https://doi.org/10.1111/j.1461-0248.2005.00792.x>
- 956 Guisan, A., Zimmermann, N.E., 2000. Predictive habitat distribution models in ecology. *Ecol. Model.*
957 135, 147–186. [https://doi.org/10.1016/S0304-3800\(00\)00354-9](https://doi.org/10.1016/S0304-3800(00)00354-9)
- 958 Hale, R., Calosi, P., McNeill, L., Mieszkowska, N., Widdicombe, S., 2011. Predicted levels of future
959 ocean acidification and temperature rise could alter community structure and biodiversity in
960 marine benthic communities. *Oikos* 120, 661–674. <https://doi.org/10.1111/j.1600-0706.2010.19469.x>
- 962 Hayward, P.J., Ryland, J.S., 1995. *Handbook of the marine fauna of north-west Europe*. Oxford
963 University Press.
- 964 He, K.S., Bradley, B.A., Cord, A.F., Rocchini, D., Tuanmu, M.-N., Schmidtlein, S., Turner, W., Wegmann,
965 M., Pettorelli, N., 2015. Will remote sensing shape the next generation of species distribution
966 models? *Remote Sens. Ecol. Conserv.* 1, 4–18. <https://doi.org/10.1002/rse2.7>
- 967 Healy, T., Wang, Y., Healy, J.-A., 2002. *Muddy Coasts of the World: Processes, Deposits and Function*.
968 Elsevier.
- 969 Herman, P.M.J., Middelburg, J.J., Heip, C.H.R., 2001. Benthic community structure and sediment
970 processes on an intertidal flat: results from the ECOFLAT project. *Cont. Shelf Res., European*
971 *Land-Ocean Interaction* 21, 2055–2071. [https://doi.org/10.1016/S0278-4343\(01\)00042-5](https://doi.org/10.1016/S0278-4343(01)00042-5)

972 Herman, P.M.J., Middelburg, J.J., Van De Koppel, J., Heip, C.H.R., 1999. Ecology of Estuarine
973 Macrobenthos, in: Nedwell, D.B., Raffaelli, D.G. (Eds.), *Advances in Ecological Research*,
974 *Estuaries*. Academic Press, pp. 195–240. [https://doi.org/10.1016/S0065-2504\(08\)60194-4](https://doi.org/10.1016/S0065-2504(08)60194-4)

975 Huang, Q., Zhang, H., Chen, J., He, M., 2017. Quantile Regression Models and Their Applications: A
976 Review. *J. Biom. Biostat.* 08. <https://doi.org/10.4172/2155-6180.1000354>

977 Hughes, B., Levey, M., Brown, J.A., Fountain, M., Carlisle, A., Litvin, S., Greene, C., Heady, W.N.,
978 Gleason, M., 2014. Nursery functions of U.S. west coast estuaries: the state of knowledge for
979 juveniles of focal fish and invertebrate species.

980 Huisman, J., Olff, H., Fresco, L. f. m., 1993. A hierarchical set of models for species response analysis.
981 *J. Veg. Sci.* 4, 37–46. <https://doi.org/10.2307/3235732>

982 Husson, F., Josse, J., Le, S., Mazet, J., 2024. FactoMineR: Multivariate Exploratory Data Analysis and
983 Data Mining.

984 Jiménez-Valverde, A., Aragón, P., Lobo, J.M., 2021. Deconstructing the abundance–suitability
985 relationship in species distribution modelling. *Glob. Ecol. Biogeogr.* 30, 327–338.
986 <https://doi.org/10.1111/geb.13204>

987 Jones, C.G., Lawton, J.H., Shachak, M., 1994. Organisms as Ecosystem Engineers. *Oikos* 69, 373–
988 386. <https://doi.org/10.2307/3545850>

989 Kassambara, A., Mundt, F., 2020. factoextra: Extract and Visualize the Results of Multivariate Data
990 Analyses.

991 Kearney, M., Porter, W., 2009. Mechanistic niche modelling: combining physiological and spatial data
992 to predict species' ranges. *Ecol. Lett.* 12, 334–350. [https://doi.org/10.1111/j.1461-](https://doi.org/10.1111/j.1461-0248.2008.01277.x)
993 [0248.2008.01277.x](https://doi.org/10.1111/j.1461-0248.2008.01277.x)

994 Koenker, R., 2019. Quantile regression in r: a vignette.

995 Koenker, R., 2006. Pseudo R for Quant Reg.

996 Koenker, R., Bassett, G., 1978. Regression Quantiles. *Econometrica* 46, 33.
997 <https://doi.org/10.2307/1913643>

998 Koenker, R., code), S.P. (Contributions to C.Q., code), P.T.N. (Contributions to S.Q., code), A.Z.
999 (Contributions to dynrq code essentially identical to his dynlm, code), P.G. (Contributions to nlrq,
1000 routines), C.M. (author of several linpack, advice), B.D.R. (Initial (2001) R. port from S. (to my
1001 everlasting shame--how could I. have been so slow to adopt R. and for numerous other
1002 suggestions and useful, 2019. quantreg: Quantile Regression.

1003 Koenker, R., code), S.P. (Contributions to C.Q., code), P.T.N. (Contributions to S.Q., code), B.M.
1004 (Contributions to preprocessing, code), A.Z. (Contributions to dynrq code essentially identical
1005 to his dynlm, code), P.G. (Contributions to nlrq, routines), C.M. (author of several linpack,
1006 sparskit2), Y.S. (author of, code), V.C. (contributions to extreme value inference, code), I.F.-V.
1007 (contributions to extreme value inference, advice), B.D.R. (Initial (2001) R. port from S. (to my

1008 everlasting shame--how could I. have been so slow to adopt R. and for numerous other
1009 suggestions and useful, 2024. *quantreg: Quantile Regression*.

1010 Koenker, R., Hallock, K., 2000. Quantile regression an introduction. *J. Econ. Perspect.* 15.

1011 Koenker, R., Hallock, K.F., 2001. *Quantile Regression* 14.

1012 Koenker, R., Machado, J.A.F., 1999. Goodness of Fit and Related Inference Processes for Quantile
1013 Regression. *J. Am. Stat. Assoc.* 94, 1296–1310.
1014 <https://doi.org/10.1080/01621459.1999.10473882>

1015 Kristensen, E., Penha-Lopes, G., Delefosse, M., Valdemarsen, T., Quintana, C.O., Banta, G.T., 2012.
1016 What is bioturbation? The need for a precise definition for fauna in aquatic sciences. *Mar. Ecol.*
1017 *Prog. Ser.* 446, 285–302. <https://doi.org/10.3354/meps09506>

1018 Łapucki, T., Normant, M., 2008. Physiological responses to salinity changes of the isopod *Idotea*
1019 *chelipes* from the Baltic brackish waters. *Comp. Biochem. Physiol. A. Mol. Integr. Physiol.* 149,
1020 299–305. <https://doi.org/10.1016/j.cbpa.2008.01.009>

1021 Le Guen, C., Tecchio, S., Dauvin, J.-C., De Roton, G., Lobry, J., Lepage, M., Morin, J., Lassalle, G.,
1022 Raoux, A., Niquil, N., 2019. Assessing the ecological status of an estuarine ecosystem: linking
1023 biodiversity and food-web indicators. *Estuar. Coast. Shelf Sci.* 228, 106339.
1024 <https://doi.org/10.1016/j.ecss.2019.106339>

1025 Le Hir, M., Hily, C., 2005. Macrofaunal diversity and habitat structure in intertidal boulder fields.
1026 *Biodivers. Conserv.* 14, 233–250. <https://doi.org/10.1007/s10531-005-5046-0>

1027 Le Hir, P., Cayocca, F., Waeles, B., 2011. Dynamics of sand and mud mixtures: A multiprocess-based
1028 modelling strategy. *Cont. Shelf Res., Proceedings of the 9th International Conference on*
1029 *Nearshore and Estuarine Cohesive Sediment Transport Processes* 31, S135–S149.
1030 <https://doi.org/10.1016/j.csr.2010.12.009>

1031 L'Ebrellec, E., Dauvin, J.-C., Bacq, N., 2019. Macrobenthos en estuaire et baie de Seine : mise à jour
1032 de la base de données MABES. Rapport d'étude réalisé par le GIP Seine-Aval. GIP Seine Aval.

1033 Lehuen, A., Oulhen, R.-M., Zhou, Z., de Smit, J., van Ijzerloo, L., Cozzoli, F., Bouma, T., Orvain, F.,
1034 2024. Multispecies macrozoobenthic seasonal bioturbation effect on sediment erodibility. *J. Sea*
1035 *Res.* 201, 102525. <https://doi.org/10.1016/j.seares.2024.102525>

1036 Lemasson, A.J., Fletcher, S., Hall-Spencer, J.M., Knights, A.M., 2017. Linking the biological impacts of
1037 ocean acidification on oysters to changes in ecosystem services: A review. *J. Exp. Mar. Biol.*
1038 *Ecol.* 492, 49–62. <https://doi.org/10.1016/j.jembe.2017.01.019>

1039 Lesourd, S., Lesueur, P., Brun-Cottan, J.C., Garnaud, S., Poupinet, N., 2003. Seasonal variations in the
1040 characteristics of superficial sediments in a macrotidal estuary (the Seine inlet, France). *Estuar.*
1041 *Coast. Shelf Sci.* 58, 3–16. [https://doi.org/10.1016/S0272-7714\(02\)00340-2](https://doi.org/10.1016/S0272-7714(02)00340-2)

- 1042 Lesourd, S., Lesueur, P., Fisson, C., Dauvin, J.-C., 2016. Sediment evolution in the mouth of the Seine
1043 estuary (France): A long-term monitoring during the last 150years. *Comptes Rendus Geosci.*
1044 348, 442–450. <https://doi.org/10.1016/j.crte.2015.08.001>
- 1045 Li, B., Cozzoli, F., Soissons, L.M., Bouma, T.J., Chen, L., 2017. Effects of bioturbation on the erodibility
1046 of cohesive versus non-cohesive sediments along a current-velocity gradient: A case study on
1047 cockles. *J. Exp. Mar. Biol. Ecol.* 496, 84–90. <https://doi.org/10.1016/j.jembe.2017.08.002>
- 1048 Madeira, D., Fernandes, J.F., Jerónimo, D., Martins, P., Ricardo, F., Santos, A., Domingues, M.R., Diniz,
1049 M.S., Calado, R., 2021. Salinity shapes the stress responses and energy reserves of marine
1050 polychaetes exposed to warming: From molecular to functional phenotypes. *Sci. Total Environ.*
1051 795, 148634. <https://doi.org/10.1016/j.scitotenv.2021.148634>
- 1052 Mahony, K.E., Egerton, S., Lynch, S.A., Blanchet, H., Goedknecht, M.A., Groves, E., Savoye, N., de
1053 Montaudouin, X., Malham, S.K., Culloty, S.C., 2022. Drivers of growth in a keystone fished
1054 species along the European Atlantic coast: The common cockle *Cerastoderma edule*. *J. Sea
1055 Res.* 179, 102148. <https://doi.org/10.1016/j.seares.2021.102148>
- 1056 Malham, S.K., Hutchinson, T.H., Longshaw, M., 2012. A review of the biology of European cockles (
1057 *Cerastoderma* spp.). *J. Mar. Biol. Assoc. U. K.* 92, 1563–1577.
1058 <https://doi.org/10.1017/S0025315412000355>
- 1059 Matos, F.L., Vaz, N., Picado, A., Dias, J.M., Maia, F., Gaspar, M.B., Magalhães, L., 2023. Assessment
1060 of Habitat Suitability for Common Cockles in the Ria the Aveiro Lagoon Under Average and
1061 Projected Environmental Conditions. *Estuaries Coasts* 46, 512–525.
1062 <https://doi.org/10.1007/s12237-022-01136-z>
- 1063 Medeiros, I.P.M., Faria, S.C., Souza, M.M., 2020. Osmoionic homeostasis in bivalve mollusks from
1064 different osmotic niches: Physiological patterns and evolutionary perspectives. *Comp. Biochem.*
1065 *Physiol. A. Mol. Integr. Physiol.* 240, 110582. <https://doi.org/10.1016/j.cbpa.2019.110582>
- 1066 Melo-Merino, S.M., Reyes-Bonilla, H., Lira-Noriega, A., 2020. Ecological niche models and species
1067 distribution models in marine environments: A literature review and spatial analysis of evidence.
1068 *Ecol. Model.* 415, 108837. <https://doi.org/10.1016/j.ecolmodel.2019.108837>
- 1069 Mengual, B., Le Hir, P., Rivier, A., Caillaud, M., Grasso, F., 2020. Numerical modeling of bedload and
1070 suspended load contributions to morphological evolution of the Seine Estuary (France). *Int. J.
1071 Sediment Res.* 36, 723–735. <https://doi.org/10.1016/j.ijsrc.2020.07.003>
- 1072 Morelle, J., Claquin, P., Orvain, F., 2020. Evidence for better microphytobenthos dynamics in mixed
1073 sand/mud zones than in pure sand or mud intertidal flats (Seine estuary, Normandy, France).
1074 *PLOS ONE* 15, e0237211. <https://doi.org/10.1371/journal.pone.0237211>
- 1075 Morelle, J., Schapira, M., Orvain, F., Riou, P., Lopez, P.J., Duplessix, O., Rabiller, E., Maheux, F.,
1076 Simon, B., Claquin, P., 2018. Annual Phytoplankton Primary Production Estimation in a
1077 Temperate Estuary by Coupling PAM and Carbon Incorporation Methods. *Estuaries Coasts* 41,
1078 1337–1355. <https://doi.org/10.1007/s12237-018-0369-8>

- 1079 Murray, N.J., Phinn, S.R., DeWitt, M., Ferrari, R., Johnston, R., Lyons, M.B., Clinton, N., Thau, D., Fuller,
1080 R.A., 2019. The global distribution and trajectory of tidal flats. *Nature* 565, 222–225.
1081 <https://doi.org/10.1038/s41586-018-0805-8>
- 1082 Ong, E.Z., Briffa, M., Moens, T., Van Colen, C., 2017. Physiological responses to ocean acidification
1083 and warming synergistically reduce condition of the common cockle *Cerastoderma edule*. *Mar.*
1084 *Environ. Res.* 130, 38–47. <https://doi.org/10.1016/j.marenvres.2017.07.001>
- 1085 Orvain, F., Lefebvre, S., Montepini, J., Sébire, M., Gangnery, A., Sylvand, B., 2012. Spatial and temporal
1086 interaction between sediment and microphytobenthos in a temperate estuarine macro-intertidal
1087 bay. *Mar. Ecol. Prog. Ser.* 458, 53–68. <https://doi.org/10.3354/meps09698>
- 1088 Peteiro, L.G., Woodin, S.A., Wethey, D.S., Costas-Costas, D., Martínez-Casal, A., Olabarria, C.,
1089 Vázquez, E., 2018. Responses to salinity stress in bivalves: Evidence of ontogenetic changes
1090 in energetic physiology on *Cerastoderma edule*. *Sci. Rep.* 8, 8329.
1091 <https://doi.org/10.1038/s41598-018-26706-9>
- 1092 Rakotomalala, C., Grangeré, K., Ubertini, M., Forêt, M., Orvain, F., 2015. Modelling the effect of
1093 *Cerastoderma edule* bioturbation on microphytobenthos resuspension towards the planktonic
1094 food web of estuarine ecosystem. *Ecol. Model.* 316, 155–167.
1095 <https://doi.org/10.1016/j.ecolmodel.2015.08.010>
- 1096 Richards, D., Lavorel, S., 2023. Niche theory improves understanding of associations between
1097 ecosystem services. *One Earth* 6, 811–823. <https://doi.org/10.1016/j.oneear.2023.05.025>
- 1098 Robinson, L.M., Elith, J., Hobday, A.J., Pearson, R.G., Kendall, B.E., Possingham, H.P., Richardson,
1099 A.J., 2011. Pushing the limits in marine species distribution modelling: lessons from the land
1100 present challenges and opportunities. *Glob. Ecol. Biogeogr.* 20, 789–802.
1101 <https://doi.org/10.1111/j.1466-8238.2010.00636.x>
- 1102 Robinson, N.M., Nelson, W.A., Costello, M.J., Sutherland, J.E., Lundquist, C.J., 2017. A Systematic
1103 Review of Marine-Based Species Distribution Models (SDMs) with Recommendations for Best
1104 Practice. *Front. Mar. Sci.* 4. <https://doi.org/10.3389/fmars.2017.00421>
- 1105 Roland, A., Ardhuin, F., 2014. On the developments of spectral wave models: numerics and
1106 parameterizations for the coastal ocean. *Ocean Dyn.* 64, 833–846.
1107 <https://doi.org/10.1007/s10236-014-0711-z>
- 1108 Saint-Béat, B., Dupuy, C., Bocher, P., Chalumeau, J., De Crignis, M., Fontaine, C., Guizien, K., Lavaud,
1109 J., Lefebvre, S., Montanié, H., Mouget, J.-L., Orvain, F., Pascal, P.-Y., Quaintenne, G.,
1110 Radenac, G., Richard, P., Robin, F., Vézina, A.F., Niquil, N., 2013. Key Features of Intertidal
1111 Food Webs That Support Migratory Shorebirds. *PLoS ONE* 8, e76739.
1112 <https://doi.org/10.1371/journal.pone.0076739>
- 1113 Santos, C., Cabral, S., Carvalho, F., Sousa, A., Goulding, T., Ramajal, J., Medeiros, J.P., Silva, G.,
1114 Angélico, M.M., Gaspar, M.B., Brito, A.C., Costa, J.L., Chainho, P., 2022. Spatial and Temporal
1115 Variations of Cockle (*Cerastoderma* spp.) Populations in Two Portuguese Estuarine Systems

- 1116 With Low Directed Fishing Pressure. *Front. Mar. Sci.* 9.
1117 <https://doi.org/10.3389/fmars.2022.699622>
- 1118 Sauriau, P.-G., Kang, C.-K., 2000. Stable isotope evidence of benthic microalgae-based growth and
1119 secondary production in the suspension feeder *Cerastoderma edule* (Mollusca, Bivalvia) in the
1120 Marennes-Oléron Bay, in: Jones, M.B., Azevedo, J.M.N., Neto, A.I., Costa, A.C., Martins, A.M.F.
1121 (Eds.), *Island, Ocean and Deep-Sea Biology, Developments in Hydrobiology*. Springer
1122 Netherlands, Dordrecht, pp. 317–329. https://doi.org/10.1007/978-94-017-1982-7_29
- 1123 Schickele, A., Leroy, B., Beaugrand, G., Goberville, E., Hattab, T., Francour, P., Raybaud, V., 2020.
1124 Modelling European small pelagic fish distribution: Methodological insights. *Ecol. Model.* 416,
1125 108902. <https://doi.org/10.1016/j.ecolmodel.2019.108902>
- 1126 Schröder, H.K., Andersen, H.E., Kiehl, K., 2005. Rejecting the mean: Estimating the response of fen
1127 plant species to environmental factors by non-linear quantile regression. *J. Veg. Sci.* 16, 373–
1128 382. <https://doi.org/10.1111/j.1654-1103.2005.tb02376.x>
- 1129 Schulz, E., Grasso, F., Le Hir, P., Verney, R., Thouvenin, B., 2018. Suspended Sediment Dynamics in
1130 the Macrotidal Seine Estuary (France): 2. Numerical Modeling of Sediment Fluxes and Budgets
1131 Under Typical Hydrological and Meteorological Conditions. *J. Geophys. Res. Oceans* 123, 578–
1132 600. <https://doi.org/10.1002/2016JC012638>
- 1133 Shi, B., Pratolongo, P.D., Du, Y., Li, J., Yang, S.L., Wu, J., Xu, K., Wang, Y.P., 2020. Influence of
1134 Macrobenthos (*Meretrix meretrix* Linnaeus) on Erosion-Accretion Processes in Intertidal Flats:
1135 A Case Study From a Cultivation Zone. *J. Geophys. Res. Biogeosciences* 125,
1136 e2019JG005345. <https://doi.org/10.1029/2019JG005345>
- 1137 Singer, A., Millat, G., Staneva, J., Kröncke, I., 2017. Modelling benthic macrofauna and seagrass
1138 distribution patterns in a North Sea tidal basin in response to 2050 climatic and environmental
1139 scenarios. *Estuar. Coast. Shelf Sci.* 188, 99–108. <https://doi.org/10.1016/j.ecss.2017.02.003>
- 1140 Srivastava, V., Lafond, V., Griess, V.C., 2019. Species distribution models (SDM): applications, benefits
1141 and challenges in invasive species management. *CABI Rev.* 2019, 1–13.
1142 <https://doi.org/10.1079/PAVSNNR201914020>
- 1143 Stephenson, F., Gladstone-Gallagher, R.V., Bulmer, R.H., Thrush, S.F., Hewitt, J.E., 2022. Inclusion of
1144 biotic variables improves predictions of environmental niche models. *Divers. Distrib.* 28, 1373–
1145 1390. <https://doi.org/10.1111/ddi.13546>
- 1146 Tecchio, S., Chaalali, A., Raoux, A., Tous Rius, A., Lequesne, J., Girardin, V., Lassalle, G., Cachera,
1147 M., Riou, P., Lobry, J., Dauvin, J.-C., Niquil, N., 2016. Evaluating ecosystem-level
1148 anthropogenic impacts in a stressed transitional environment: The case of the Seine estuary.
1149 *Ecol. Indic.* 61, 833–845. <https://doi.org/10.1016/j.ecolind.2015.10.036>
- 1150 Thomas, Y., Bacher, C., 2018. Assessing the sensitivity of bivalve populations to global warming using
1151 an individual-based modelling approach. *Glob. Change Biol.* 24, 4581–4597.
1152 <https://doi.org/10.1111/gcb.14402>

- 1153 Thrush, S., Hewitt, J., Herman, P., Ysebaert, T., 2005. Multi-scale analysis of species-environment
1154 relationships. *Mar. Ecol.-Prog. Ser.* 302, 13–26. <https://doi.org/10.3354/Meps302013>
- 1155 Thrush, S., Hewitt, J., Norkko, A., Nicholls, P., Funnell, G., Ellis, J., 2003. Habitat change in estuaries:
1156 predicting broad-scale responses of intertidal macrofauna to sediment mud content. *Mar. Ecol.*
1157 *Prog. Ser.* 263, 101–112. <https://doi.org/10.3354/meps263101>
- 1158 Ubertini, M., Lefebvre, S., Gangnery, A., Grangeré, K., Le Gendre, R., Orvain, F., 2012. Spatial
1159 Variability of Benthic-Pelagic Coupling in an Estuary Ecosystem: Consequences for
1160 Microphytobenthos Resuspension Phenomenon. *PLoS ONE* 7, e44155.
1161 <https://doi.org/10.1371/journal.pone.0044155>
- 1162 Underwood, A.J., Chapman, M.G., 1996. Scales of spatial patterns of distribution of intertidal
1163 invertebrates. *Oecologia* 107, 212–224. <https://doi.org/10.1007/BF00327905>
- 1164 Van Colen, C., Montserrat, F., Vincx, M., Herman, P.M.J., Ysebaert, T., Degraer, S., 2010.
1165 Macrobenthos recruitment success in a tidal flat: Feeding trait dependent effects of disturbance
1166 history. *J. Exp. Mar. Biol. Ecol.* 385, 79–84. <https://doi.org/10.1016/j.jembe.2010.01.009>
- 1167 Van Der Wal, D., Herman, P., Forster, R., Ysebaert, T., Rossi, F., Knaeps, E., Plancke, Y., Ides, S.,
1168 2008. Distribution and dynamics of intertidal macrobenthos predicted from remote sensing:
1169 response to microphytobenthos and environment. *Mar. Ecol. Prog. Ser.* 367, 57–72.
1170 <https://doi.org/10.3354/meps07535>
- 1171 Van Der Wal, D., Wielemaker-van Den Dool, A., Herman, P.M.J., 2010. Spatial Synchrony in Intertidal
1172 Benthic Algal Biomass in Temperate Coastal and Estuarine Ecosystems. *Ecosystems* 13, 338–
1173 351. <https://doi.org/10.1007/s10021-010-9322-9>
- 1174 Van Der Wal, D., Ysebaert, T., Herman, P.M.J., 2017. Response of intertidal benthic macrofauna to
1175 migrating megaripples and hydrodynamics. *Mar. Ecol. Prog. Ser.* 585, 17–30.
1176 <https://doi.org/10.3354/meps12374>
- 1177 Vera, M., Wilmes, S.B., Maroso, F., Hermida, M., Blanco, A., Casanova, A., Iglesias, D., Cao, A., Culloty,
1178 S.C., Mahony, K., Orvain, F., Bouza, C., Robins, P.E., Malham, S.K., Lynch, S., Villalba, A.,
1179 Martínez, P., 2023. Heterogeneous microgeographic genetic structure of the common cockle
1180 (*Cerastoderma edule*) in the Northeast Atlantic Ocean: biogeographic barriers and
1181 environmental factors. *Heredity* 131, 292–305. <https://doi.org/10.1038/s41437-023-00646-1>
- 1182 Warren, D.L., Seifert, S.N., 2011. Ecological niche modeling in Maxent: the importance of model
1183 complexity and the performance of model selection criteria. *Ecol. Appl.* 21, 335–342.
1184 <https://doi.org/10.1890/10-1171.1>
- 1185 Ysebaert, T., Herman, P.M.J., 2002. Spatial and temporal variation in benthic macrofauna and
1186 relationships with environmental variables in an estuarine, intertidal soft-sediment environment.
1187 *Mar. Ecol. Prog. Ser.* 244, 105–124. <https://doi.org/10.3354/meps244105>

- 1188 Ysebaert, T., Meire, P., Herman, P.M.J., Verbeek, H., 2002. Macrobenthic species response surfaces
1189 along estuarine gradients: prediction by logistic regression. *Mar. Ecol. Prog. Ser.* 225, 79–95.
1190 <https://doi.org/10.3354/meps225079>
- 1191 Zhou, Z., Bouma, T.J., Fivash, G.S., Ysebaert, T., van IJzerloo, L., van Dalen, J., van Dam, B., Walles,
1192 B., 2022. Thermal stress affects bioturbators' burrowing behavior: A mesocosm experiment on
1193 common cockles (*Cerastoderma edule*). *Sci. Total Environ.* 824, 153621.
1194 <https://doi.org/10.1016/j.scitotenv.2022.153621>
- 1195
- 1196

1197 Reference list

1198 Figure 1 Maps showing the habitats defined in the dataset of the study area. Dots represent the
1199 location of the biological samples.

1200 Figure 2: Principal Components Analysis (PCA) variable correlation plot with the abiotic factors'
1201 contributions in bar plots for each axis. The red dotted line represents the mean contribution for all
1202 factors.

1203 Figure 3: Example of modelled vs observed biomass data plotted for each model functions. The
1204 selected predictors were the daily maximum current speed [m.s^{-1}], daily salinity range and inundation
1205 time [% in this example]. The black line represents the 1:1 ratio, quantiles 0.5 in blue, 0.9 in green, 0.95
1206 in orange and 0.975 in red.

1207 Figure 4: First row – (%) Projection on the three abiotic factor axes with observation compared to the
1208 modelled quantiles for the daily maximum current speed (m.s^{-1}), the daily salinity range and the
1209 inundation time (A1). The second column displays the predicted/observed validation plot associated to
1210 this model (A2). Second row – Same figure with the 2nd model with projection on the three abiotic factor
1211 axes: daily maximum current speed (m.s^{-1}), inundation time (%) and mud content (%) (B1); The second
1212 column displays the predicted/observed validation plot associated (B2). Black dots in A1 and B1
1213 represents the observed data; lines the modelled quantiles; Coloured dots in A2 and B2 correspond to
1214 each decile of the modelled distribution and its corresponding observed, black line represents the 1:1
1215 ratio. Quantiles are colour coded as 0.5 in blue, 0.9 in green, 0.95 in orange and 0.975 in red.

1216 Figure 5: A: Daily maximum current speed [m.s^{-1}] & daily salinity range & inundation time [%] model
1217 suitability index applied on the Seine estuary over the five periods. B: Abiotic factors and resulting model
1218 at 97.5th centile suitability index per period and per area for all SDM models with a 95% confidence
1219 interval.

1220 Figure 6: A: Daily maximum current speed [m.s^{-1}] & inundation time [%] & mud content [%] model
1221 suitability index applied on the Seine estuary over the five periods. B: Abiotic factors and resulting model
1222 at 97.5th centile suitability index per period and per area for all SDM models with a 95% confidence
1223 interval.

1224 Figure 7: Seine model daily maximum current speed (m.s^{-1}) & daily salinity range & inundation time
1225 (%) projection on the three abiotic factor axes with data from Scheldt basins in blue dots for
1226 Oosterschelde and red dots for Westerschelde (A) and the predicted/observed validation plot computed
1227 on Scheldt application of the model parametrized in the Seine estuary (B). Black dots in A represents
1228 the observed data that were used for parameterisation (in the Seine estuary) while green dots are the
1229 data from the Scheldt basins; lines represent the model quantiles. Coloured dots in B correspond to each
1230 decile of the modelled distribution and its corresponding observed, black line represents the 1:1 ratio.
1231 Quantiles are colour coded as 0.5 in blue, 0.9 in green, 0.95 in orange and 0.975 in red.

1232

1233 Table list

1234 Table 1 List of types of models tested

1235 Table 2 Principal Components Analysis (PCA) scores for abiotic factors. Cos2, cosine squared of the
1236 variables, represents the quality of the representation of the variables on the PCA graph; Contribution
1237 represents the contributions (in percentage) of the variables to the principal components. The
1238 contribution of a variable to a given principal component: $(\text{Variable.cos2} * 100) / (\text{total cos2 of the}$
1239 $\text{component})$.

1240 Table 3 AICc comparison for all models computed, according to the quantile, the type of equation
1241 and the response. In bold, the lower value of each model by response and quantile.

1242 Table 4: Coefficient of the models computed with gaussian equation (Equation 1), by quantile and
1243 response.

1244